THE ASTROPHYSICAL JOURNAL, 318:337–355, 1987 July 1

THE DISTRIBUTION OF ROTATIONAL VELOCITIES FOR LOW-MASS STARS IN THE PLEIADES[1]

JOHN R. STAUFFER[2]
Dominion Astrophysical Observatory[3]

AND

LEE W. HARTMANN
Smithsonian Astrophysical Observatory
Received 1986 August 26; accepted 1986 December 10

ABSTRACT

We present new observations which extend our previous photometric and spectroscopic studies of late-type members of the Pleiades. The original finding of rapid rotators among K and M dwarfs and a minimum in the rotational velocity distribution at type G is confirmed through the inclusion of rotation estimates for additional members. As noted in Paper I of this series, the presence of a large number of late-type stars with $v \sin i \approx 100$ km s^{-1}, and the absence of comparable rotational velocities in both younger and older groups of stars, indicate that low-mass stars spin up appreciably during pre–main-sequence contraction, and spin down very rapidly once on the main sequence. We show that the wide range of angular momenta exhibited by Pleiades K and M dwarfs is not necessarily produced by a combination of main-sequence spin-down and a large age spread. This distribution can also result from a plausible spread in initial angular momenta, coupled with initial main-sequence spin-down rates that are only weakly dependent on rotation.

We have also refined our determination of the distribution of rotational velocity as a function of $V-I$ color by consideration of the differential reddening in the Pleiades. Our new reddening estimates for late-type members of the cluster confirm Breger's finding of large extinctions confined to a small region in the southern portion of the Merope nebula.

Subject headings: clusters: open — stars: rotation

I. INTRODUCTION

The rotational velocity characteristics of stars more massive than the Sun are now fairly well understood as the result of observational programs carried out during the 1950s and 1960s (Slettebak 1954, 1955; Abt and Hunter 1962; Kraft 1967; Wilson 1966). These authors showed that high-mass stars ($M > 2\ M_\odot$) typically have rotational velocities on the order of 100 km s^{-1}, while low-mass stars ($M < 1\ M_\odot$) normally have rotational velocities less than 10 km s^{-1}. More recent studies by Smith (1979), Baliunas *et al.* (1983), Soderblom (1983, 1985), and Gray (1984) confirm that late-type, old field dwarfs with few exceptions are slow rotators. The K dwarfs in the Hyades also all appear to have rotational velocities less than 10 km s^{-1} (Baliunas *et al.* 1983; Radick *et al.* 1986; Stauffer, Hartmann, and Latham 1986).

The large difference in the rotational velocities of high-mass and low-mass main-sequence stars disappears when one considers young star clusters. Stauffer *et al.* (1984, hereafter SHSB) and Stauffer *et al.* (1985, hereafter SHBJ) have recently shown that K and M dwarfs in the Pleiades and α Per clusters have rotational velocities ranging from less than 10 km s^{-1} to nearly 150 km s^{-1}. Approximately a third of the late-type stars in each cluster have rotational velocities greater than 40 km s^{-1}. Many of the late-type rapid rotators are heavily spotted, photometric variables (van Leeuwen and Alphenaar 1982; Stauffer 1984; Stauffer *et al.* 1986), and most of these stars have moderately strong chromospheric emission (Hartmann and Stauffer 1987). The Hα emission-line profiles for a few of the rapid rotators are suggestive of mass loss via a wind (SHSB; Marcy, Duncan, and Cohen 1985, hereafter MDC). MDC infer mass-loss rates on the order of $10^{-9}\ M_\odot$ yr^{-1}, and an angular momentum spin-down time scale of order 10^7 years for HII 1883, the most rapidly rotating Pleiades K dwarf (HII refers to the second list in Hertzsprung 1947, sometimes referred to in previous work as Hz).

The difference in rotational velocity character between the young and old low-mass stars can be reasonably ascribed to an evolutionary sequence. Low-mass, pre–main-sequence stars on Hayashi tracks typically have relatively low rotational velocities, $v \sin i < 20$ km s^{-1} (Vogel and Kuhi 1981; Hartmann *et al.* 1986, hereafter HHSM; Bouvier *et al.* 1986). The surface rotational velocities of these stars increase significantly during pre–main-sequence contraction because of the large decrease in their moment of inertia. Once on the main sequence, however, angular momentum loss resulting from magnetically coupled winds quickly decreases the surface rotational velocities. This scenario is supported by the independent theoretical calculations of Endal and Sofia (1981), whose models predict a rotational velocity for the Sun of $v_{\rm rot} \approx 70$ km s^{-1} upon arrival on the main sequence, with a spin-down to $v_{\rm rot} \approx 10$ km s^{-1} in a few times 10^7 yr.

Our previous studies were aimed primarily at determining the general spectral type range over which rapid rotation occurs in the α Per and Pleiades clusters and at determining the range in rotational velocity for late-type dwarfs in these

[1] Research reported here used the Multiple Mirror Telescope Observatory, a joint facility of the Smithsonian Institution and the University of Arizona.

[2] Visiting Astronomer, Kitt Peak National Observatory, which is operated by the Association of Universities for Research in Astronomy, Inc., under contract with the National Science Foundation.

[3] New address: NASA/Ames Research Center; and Lick Observatory, University of California at Santa Cruz.

clusters. In order to obtain more quantitative knowledge of the spin-down mechanism, we are now attempting to determine the distribution of rotational velocities as a function of spectral type in these two clusters. Here we present new rotational velocities for an additional set of stars in the Pleiades cluster. We believe the data support a view that the decrease in surface rotational velocities due to magnetic braking in the low-mass stars affects primarily the outer convective envelope. Therefore, G dwarfs, with thin convective envelopes, are spun down quickly and appear as slow rotators in the Pleiades, whereas many of the K and M dwarfs are rapid rotators.

Breger's (1985) study of the reddening toward stars in the vicinity of the Pleiades affects our program in one small, but important, way. Two of the six stars for which Breger derived relatively large reddenings have been identified by SHSB as rapid rotators. With the reddening corrections advocated by Breger, these two stars become the bluest late-type rapid rotators in the Pleiades. We have, therefore, reanalyzed the available spectral type and color data for late-type Pleiades members, and derived new reddening estimates. New photometry for a small number of stars, as well as a compilation of Hα equivalent widths for Pleiades dwarfs, is also presented.

TABLE 1

SPECTROSCOPIC ROTATIONAL VELOCITIES

Star (1)	$V-I$ (2)	$v \sin i$ (3)	R (4)	Notes (5)	Star (1)	$V-I$ (2)	$v \sin i$ (3)	R (4)	Notes (5)
HII 97	1.06	<10	18		HII 1015	0.50	18	10	4
HII 102	0.64	20	4		HII 1081	1.73	<10	8	
HII 120	0.57	11	8		HII 1095	0.74	<10	14	
HII 133	1.56	19	5		HII 1101	0.49	18	8	
HII 134A	1.95	70	...	1, 2	HII 1103	1.76	18	7	
HII 134B	1.95	65	...	1, 2	HII 1110	1.22	11	5	
HII 146	1.64	<10	7		HII 1124	0.88	<10	9	
HII 152	0.52	11	7		HII 1207	0.50	<10	12	
HII 173	0.70	10	8		HII 1215	0.49	<10	11	
HII 189	1.46	<10	6		HII 1275	0.67	<10	10	
HII 193	0.66	14	8		HII 1298	0.89	<10	11	
HII 212	1.58	10	7		HII 1332	0.91	<10	10	
HII 233	0.40	13	10	3	HII 1454	1.05	<10	16	
HII 248	0.65	12	10		HII 1512	1.23	<10	12	
HII 250	0.52	<10	11		HII 1514	0.51	15	10	
HII 263	0.76	14	8		HII 1532	1.44	50	3	
HII 293	0.56	<10	12		HII 1593	0.62	<10	8	
HII 296	0.72	15	12		HII 1613	0.38	19	8	3
HII 303A	0.85	17	9	1	HII 1653	1.32	21	5	5
HII 303B	0.85	23	5	1	HII 1726	0.41	12	12	3
HII 335	1.47	73	2.5		HII 1756	1.45	<10	9	
HII 347	1.77	75	...	2	HII 1776	0.58	13	11	
HII 380	1.21	<10	9		HII 1785	...	<10	8	
HII 405	0.40	20	6	3	HII 1794	0.47	13	12	
HII 430	0.66	<10	10		HII 1856	0.42	16	9	3
HII 451	1.25	<10	7		HII 1924	0.46	14	9	
HII 489	0.51	17	9		HII 2016	1.29	10	10	
HII 514	0.55	12	7		HII 2106	0.75	10	12	
HII 522	0.80	<10	13		HII 2172	0.46	11	10	
HII 559	1.21	65	...	2	HII 2193	1.56	23	6	
HII 624	1.99	16	7		HII 2208	1.71	73	2.5	
HII 625	1.27	50	2		HII 2209	1.65	<10	8	
HII 636	0.93	<10	14		HII 2341	0.53	<10	10	
HII 673	2.26	14	4	4	HII 2366	0.66	<10	12	
HII 676	1.34	10	9		HII 2368	...	26	6	
HII 739	0.51	14	11		HII 2407	0.82	<10	8	
HII 740	1.10	14	13		HII 2462	0.66	10	8	
HII 746	0.68	<10	11		HII 2548	1.46	<10	9	
HII 762	1.55	<10	9		HII 2588	1.20	<10	10	
HII 793	1.59	<10	10		HII 2644	0.56	<10	7	
HII 799	1.39	<10	12		HII 2741	0.94	11	7	
HII 879	1.01	<10	13		HII 2927	1.44	95	2	
HII 883	1.11	<10	12		HII 2966	1.80	<10	6	
HII 890	1.72	<10	6		HII 3019	...	<10	13	
HII 915	1.35	12	5		HII 3030	1.46	<10	9	
HII 916	0.75	<10	13	3	MT 41	2.17	15	2.5	6
HII 923	0.48	18	9		T 18A	2.66	65	...	2, 6
HII 930	1.55	15	7		T 18B	2.66	50	...	2, 6
HII 974	1.45	<10	7		T 42B	2.04	24	5	6
HII 996	0.48	11	9						

NOTES.—(1) Member of a visual binary. $V-I$ is that of the pair. (2) Value of $v \sin i$ estimated from fit to Hα profile (see SHSB). (3) $V-I$ not observed. Estimate of $V-I$ derived from $B-V$ colors. (4) Radial velocity probably inconsistent with Pleiades membership. (5) May be an SB2. (6) MT = McCarthy and Treanor 1968; T = Tonantzintla (old numbering system; see Haro, Chavira, and Gonzalez 1982).

These data are used to examine the location of the rapid rotators in color-magnitude diagrams and the correlation between chromospheric activity and rotation.

II. OBSERVATIONAL DATA

a) Rotational Velocities

The stars observed spectroscopically for this program were selected from our previously published photometric surveys of the cluster (Stauffer 1982, 1984). The selection criteria for this season gave highest weight to stars with peculiar colors in the $B-V$, $V-I$ color-color diagram, and to stars with $V < 14$ mag. Mathieu (1985) obtained spectra for a number of Pleiades stars for another program. We have analyzed his spectra for rotational velocities, and include the results here. In all, new spectra were obtained for 100 stars, 70 of which had no previously published spectroscopic rotational velocity estimates.

All of the spectra were obtained with either the 1.5 m telescope or the Multiple Mirror Telescope on Mount Hopkins. The echelle spectrograph (Chaffee 1974) and photon-counting, intensified Reticon (Latham 1981) utilized for the previous cluster rotational velocity papers remain essentially unchanged. The instrumental resolution of the system is about 0.1 Å, and the observed wavelength regions were 5175–5225 and 6540–6590 Å. Typical spectra are shown in SHSB and SHBJ. Radial and rotational velocities for the program stars were derived via a cross-correlation technique described elsewhere (Tonry and Davis 1979; HHSM). The radial velocities will be reported by Mathieu (1986).

A list of the newly derived spectroscopic data is provided in Table 1. Column (1) there is the Hertzsprung (1947) number for the star or an alternative designation as described in the notes to the table; column (2) is the observed $V-I$ color, generally from Stauffer (1984) or references therein; column (3) provides the rotational velocities; column (4) is the R number for the highest signal-to-noise spectrum (where R is the ratio of the amplitude of the cross-correlation peak to the rms amplitude of the antisymmetric component of the correlation; see Tonry and Davis 1979); and column (5) provides a few comments on these results. According to HHSM, an average error estimate for the rotational velocities should be approximately $\pm v \sin i/2(1 + R)$. For reference, note that Pleiades stars of spectral types K0 and M0 have observed $V-I$ colors of approximately 0.75 and 1.70, respectively.

b) Photometry

Optical photometry was obtained for a sample of Pleiades stars during 1985 November using the Kitt Peak 1.3 m telescope. As with the previously reported photometry (Stauffer 1982, 1984), an RCA 31034A GaAs phototube, a $BVRI$ filter set, and the MkII computer-controlled photometer were used. Extinction corrections were derived each night; standard stars were chosen from the lists of Kron, Gascoigne, and White (1957), Landolt (1973), and Eggen (1975). Standard reduction procedures were followed.

Conditions were good for two nights of the observing run (it rained or snowed the other eight), and the photometry obtained should generally have 1 σ errors of 0.01 mag based on the scatter in the standard star photometry and on a comparison of the stars in common with Johnson and Mitchell (1958). The new data are provided in Table 2, which lists the star's name, the V, $B-V$, $V-R$, $R-I$, and $V-I$ magnitudes, and the number N of times the star was observed. We also attempted to derive light curves for photometric variables among the late-type Pleiades members in 1983 December, again using the 1.3 m telescope and MkII photometer. The weather conditions were not conducive to that purpose, and we did not obtain data adequate to derive periods for any of the program stars. A few of the stars were sufficiently "active" to allow us to estimate the amplitude of their variability. These estimates are provided in Table 3.

TABLE 2

NEW PHOTOMETRY FOR PLEIADES MEMBERS

Star	V	$B-V$	$V-R$	$R-I$	$V-I$	N
HII 102	10.52	0.71	0.33	0.31	0.64	1
HII 120	10.84	0.70	0.30	0.27	0.57	1
HII 134	14.37	1.47	1.12	0.83	1.95	1
HII 152	10.73	0.69	0.27	0.25	0.52	1
HII 193	11.30	0.79	0.35	0.31	0.66	1
HII 248	11.02	0.77	0.35	0.30	0.65	1
HII 250	10.70	0.67	0.27	0.25	0.52	1
HII 263	11.63	0.88	0.42	0.34	0.76	1
HII 293	10.79	0.70	0.29	0.27	0.56	1
HII 303ab	10.48	0.88	0.46	0.39	0.85	1
HII 324	12.87	1.06	0.60	0.46	1.06	2
HII 489	10.42	0.62	0.26	0.25	0.51	1
HII 514	10.73	0.70	0.29	0.26	0.55	1
HII 996	10.42	0.63	0.23	0.25	0.48	1
HII 1015	10.54	0.65	0.25	0.25	0.50	1
HII 1095	11.83	0.92	0.41	0.33	0.74	1
HII 1101	10.25	0.61	0.24	0.25	0.49	1
HII 1207	10.51	0.64	0.25	0.25	0.50	1
HII 1514	10.53	0.66	0.26	0.25	0.51	1
HII 1593	11.15	0.77	0.33	0.29	0.62	1
HII 1794	10.40	0.62	0.23	0.24	0.47	1
HII 1924	10.33	0.61	0.22	0.24	0.46	1
HII 2027	10.92	0.85	0.39	0.32	0.71	3
HII 2106	11.54	0.87	0.40	0.35	0.75	1
HII 2172	10.44	0.62	0.23	0.23	0.46	1
HII 2341	10.93	0.72	0.28	0.25	0.53	1
HII 2366	11.49	0.82	0.37	0.29	0.66	1
HII 2644	11.09	0.77	0.30	0.26	0.56	1
HII 3030	14.03	1.39	0.86	0.60	1.46	1

c) Hα Equivalent Widths

During the course of the last several observing seasons, we have obtained spectra covering Hα for a large number of late-type Pleiades stars. Equivalent widths for Hα measured from these spectra may be useful to those wishing to compare low-mass T Tauri star emission strengths to similar data for somewhat older stars, or to those wishing to compare field dMe stars to young cluster M dwarfs. We have reported some of the Hα data in two previous papers (Stauffer 1980, 1982). We

TABLE 3

VARIABLE STARS

Star	Range in V	Number of Observations
HII 296	11.46–11.53	13
HII 324	12.92–13.01	15
HII 738	12.31–12.36	13
HII 1305	13.48–13.54	12
HII 2208	14.37–14.45	11
HII 2244	12.63–12.68	13
HII 2927	13.93–14.02	10

TABLE 4

Hα Equivalent Widths

Star	$R-I$	Hα[a]	Star	$R-I$	Hα[a]
HII 34	0.34	−0.55	A28	1.21	4.0
HII 191	0.72	1.8	ALR 929	1.06	4.2
HII 324	0.47	0.6	B173	0.93	3.4
HII 357	0.59	1.0	B179	1.19	8.1
HII 451	0.52	0.3	B201	1.35	7.5
HII 624	0.87	2.7	B214	1.35	7.0
HII 625	0.55	−0.36	B363	1.14	5.0
HII 636	0.40	−0.48	J8	1.01	4.2
HII 686	0.58	2.5	JS 26	1.29	9.2
HII 882	0.50	1.1	JS 27	1.39	11.4
HII 1100	0.47	0.0	MT 41	1.01	3.3
HII 1124	0.39	−0.33	MT 61	1.05	3.4
HII 1173	0.83	2.0	T2B	1.32	8.1
HII 1275	0.30	−0.79	T6	1.44	12.7
HII 1286	1.04	1.5	T6B	1.33	9.5
HII 1298	0.38	−0.47	T18B	1.30	5.4
HII 1321	1.04	3.2	T23	1.34	8.0
HII 1332	0.38	−0.47	T35B	1.26	8.6
HII 1348	0.51	−0.16	T40	1.18	3.9
HII 1355	0.75	1.3	T42B	0.93	3.5
HII 1454	0.44	−0.20	T45	0.67	1.7
HII 1531	0.56	0.9	T69	1.05	2.8
HII 1883	0.46	5.5	T77	1.43	8.9
HII 2244	0.44	0.6	T86	1.06	1.8
HII 2278	0.33	−0.61	T105	1.17	6.3
HII 2311	0.30	−0.82	T150	0.95	2.8
HII 2588	0.51	0.6			
HII 2601	0.99	2.4	T151	0.71	2.1
HII 2602	1.06	3.4	T154	1.07	4.0
HII 2966	0.79	0.8	T155	1.36	17.7
HII 3163	0.47	1.1	T160	0.78	2.8
A23	1.13	5.2			

[a] Equivalent widths in angstroms.

present in Table 4 a complete list of our Hα equivalent width data. Where we have multiple observations, the value given is the average.

A plot of Hα equivalent width versus $R-I$ for the Pleiades stars (Fig. 1) shows that these two quantities are highly correlated, with only some of the most rapidly rotating K dwarfs deviating significantly. Among the M dwarfs ($R-I > 0.7$), there is no obvious correlation between rotation and Hα equivalent width. This Hα diagram could be used as a membership test for late-type stars located in the direction of the Pleiades (see also Kraft and Greenstein 1969). Alternatively, similar diagrams for several clusters of different ages could be used to measure the evolution of chromospheric activity as a function of spectral type and age for late-type stars, as has been done previously with Ca II H and K emission (Soderblom 1985; Skumanich 1972). A similar Hα versus $R-I$ diagram for field M dwarfs is provided by Stauffer and Hartmann (1986).

d) New Data for Individual Stars of Interest

A few of the stars observed during the past two seasons deserve special comment. We provide these comments here.

T18A, B.—This star has had more detected flare events than any other Pleiades member (Haro, Chavira, and Gonzales 1982). It is a visual binary, with separation about 3″ and nearly equal brightness components (Stauffer 1984). Jones (1981) derives a 93% probability that it is a Pleiades member based on his proper-motion survey of flare stars toward the Pleiades. In a V versus $V-I$ diagram, however, each component of the binary is located about 1.3 mag above the Pleiades main sequence. Therefore, Pleiades membership cannot be considered certain. The new echelle spectra allow us to measure radial velocities for the stars via fits to their Hα emission pro-

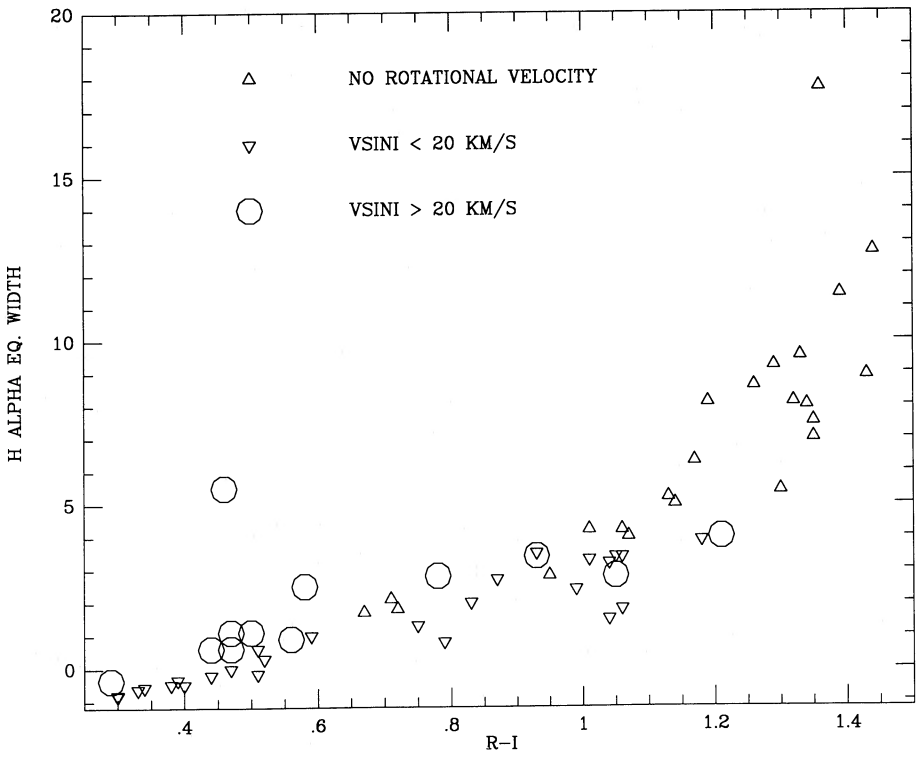

FIG. 1.—Chromospheric activity of Pleiades K and M dwarfs as a function of observed $R-I$, except for HII 625, where a large reddening correction has been applied to the observed $R-I$ (see § II).

files, yielding $cz = 11.5$ and 3.1 km s^{-1}, with a probable error of about 5 km s^{-1}. These velocities are consistent with the Pleiades mean radial velocity of $\langle cz \rangle = 5.1$ km s^{-1} and inconsistent with membership in the Hyades (for which $\langle cz \rangle \approx 40$ km s^{-1}). Thus, the case for T18A, B being Pleiades members is now improved, and the large displacement above the main sequence must be explained either as due to each of the visual components being multiple or to T18 being younger than the majority of the Pleiades stars (and thus higher up on its pre–main-sequence evolutionary track).

HII 134a, b.—SHSB gave $v \sin i \approx 40$ km s^{-1} for this "star," but noted that the spectrum was noisy. With better seeing we have identified the star as a visual binary (separation about 2″), both members of which are rapid rotators with $v \sin i = 65$–70 km s^{-1} as estimated from the width of their Hα emission profiles. Kraft and Lynds have also identified this star as a visual binary (Landolt 1979).

HII 173.—This star was noted as a double-lined spectroscopic binary in SHSB. We now have several spectra confirming that identification, and Mermilliod (1984) has also noted the star to be an SB2.

HII 296.—According to SHSB, the spectroscopic rotational velocity for this G dwarf is 17 km s^{-1}. Several new spectra obtained by us indicate that that was a slight overestimate, a better value being about 14 km s^{-1}. Comparison with HII 173 or HII 2311, which have nearly the same spectral type but are sharp-lined, illustrates the connection between rotation and activity. The two slow rotators are not photometric variables ($\Delta V < 0.03$ mag), whereas HII 296 is definitely variable, with $\Delta V \approx 0.07$ mag. Echelle spectra show that HII 296 has much weaker Hα absorption than HII 173, presumably indicating that the Hα line in HII 296 is filled in by emission.

HII 559, 883, 915, 1532 and T73.—These stars were predicted to be rapid rotators in SHSB on the basis of their colors and magnitudes (basically, they are blue in $B-V$ for their observed $V-I$ color, but they are not displaced significantly above the single-star main sequence in a color-magnitude diagram). We have now obtained echelle spectra for all five stars, and three of them do indeed have large projected rotational velocities.

III. GAS AND DUST NEAR THE PLEIADES

The presence of bright reflection nebulae around the B stars in the Pleiades suggests that there might be significant reddening along the line of sight to some or all of the Pleiades members. In fact, most Pleiades stars have a relatively small color excess, and the variation in reddening across the cluster is not particularly large. There is, however, apparently one small portion of the cluster where large reddenings are encountered. That small region is centered near the southern portion of the Merope nebula (see Fig. 1 of Andriesse, Piersma, and Witt 1977). Eggen (1950) appears to have been the first specifically to advocate relatively large color excesses in this region. Breger (1985) has combined reddening and polarization data to expand upon Eggen's proposal. Breger finds both large polarizations and large reddenings [$E(B-V) > 0.2$ mag] for six stars in the Pleiades, all of them near R.A. $3^h43^m00^s$, decl. 23°30′ (1950). That position coincides with the southern extension of the Merope nebula and the center of the molecular cloud detected in CO and OH by Federman and Willson (1984). The radial velocity of the cloud indicates that we are observing the chance passage of a small interstellar cloud through the cluster; the reflection nebula is not a remnant of the Pleiades star formation process (Arny 1977; White 1984; Castelaz, Sellgren, and Werner 1986). Thus there is no physical connection between the cloud and stellar rotation in the Pleiades. Two of the heavily reddened stars identified by Breger, HII 625 and HII 738, are classed as rapid rotators in SHSB. With the reddening advocated by Breger, these stars become the two bluest rapidly rotating late-type Pleiades members, with $V-I$(corrected) = 0.70 and 0.62, respectively. Since one of the primary differences noted between the rotational velocity characteristics of low-mass stars in the Pleiades and α Per clusters (SHBJ) was the lack of rapid rotators in the Pleiades for $0.3 < V-I < 0.9$, the reddening results may significantly affect our program. We have, therefore, derived new reddening estimates for late-type stars in the cluster.

Reddening estimates are traditionally derived by comparing observed colors with assumed intrinsic colors based on a star's spectral type. We have collected all reliable spectral classifications of which we are aware for late-type Pleiades members. Photometry is available for most of these stars. Table 5 lists the spectral types, $B-V$ colors, and references for both quantities. To derive reddenings, we have used a slightly smoothed version of the spectral type–color relation given by Fitzgerald (1970). Two caveats need to be emphasized for this technique: (1) the $B-V$ colors of late-type stars are metallicity-dependent, hence the program and calibration stars should have the same metallicities. We do not believe this is a significant problem, since Pleiades members have essentially solar abundance (Crawford and Perry 1976), and FitzGerald's stars generally should have near solar abundance, since they are primarily nearby field stars; (2) the late-type Pleiades stars are believed to be heavily spotted and chromospherically active (Stauffer 1984; Rose 1985), hence their colors and spectral characteristics differ from older, relatively unspotted stars. In particular, the $B-V$ colors for the Pleiades stars are likely to be too blue for their observed $V-I$ colors (Campbell 1984; Stauffer 1984; § IV of this paper). Spectral types estimated from blue spectra will also likely be systematically earlier than spectral types from longer wavelength spectra. For this paper we will not attempt to model the effects of spots on the properties of our program stars. Instead, we adopt a simple correction technique. The stars with early spectral types in the cluster (without outer convective envelopes, and hence without spots) are generally agreed to have a mean reddening of about 0.04 mag (Crawford and Perry 1976; Breger 1985). We assume that the late-type stars outside the region of the Merope nebula also have the same mean reddening. Using the FitzGerald standard relation, we instead derive $\langle E(B-V) \rangle = 0.08$ mag. By assumption, this difference represents the systematic error in our reddening estimates, and we have thus corrected our initial reddening estimates by 0.04 mag. The corrected reddenings are listed in column (4) of Table 5.

Our list and Breger's have 11 stars in common. For one of the stars, HII 799, there is a quite large difference in derived reddening due almost entirely to differing assumed spectral types. For the other 10 stars, the mean difference between the new reddenings and those derived by Breger is -0.04 mag. The difference essentially reflects the correction factor introduced into our reddening estimates as discussed above. For the present purpose, we will ignore that difference and simply combine the two lists without any additional zero-point corrections.

In Figure 2 we show a spatial map of all the stars for which reddening estimates are now available; the stars with $E(B-V) > 0.25$ mag are indicated by filled circles. We confirm

TABLE 5

REDDENING ESTIMATES FOR LATE-TYPE PLEIADES MEMBERS

Star	$B-V$	Spectral Type	$E(B-V)$	Reference	Star	$B-V$	Spectral Type	$E(B-V)$	Reference
81	0.92	G8	0.14	1	1275	0.93	G8	0.05	2, 6
83	1.05	K0	0.20	1	1280	1.37	K7–M0	0.00	4
133	1.35	K5.5e	0.16	1	1306	1.35	K5e	0.16	4, 5
134	1.48	K7e	0.11	1	1332	1.02	K4	−0.07	4, 6
146	1.41	K7–M0e	0.04	1	1348	1.15	K5	−0.04	4
173	0.84	K0	−0.01	2	1355	1.40	K6e	0.11	1, 3
189	1.37	K5.5e	0.18	1	1454	1.08	K5	−0.11	4
191	1.35	K7	−0.02	1, 3, 4	1485	1.32	K5e	0.13	1
212	1.37	K7e	0.00	1, 5	1512	1.26	K6	−0.03	4
296	0.84	G8	0.06	2	1531	1.27	K7–M0e	−0.10	3
335	1.26	K5e	0.07	1, 5	1553	1.09	K2.5e	0.13	5
347	1.41	K7e	0.04	1, 3, 4	1593	0.77	G6	0.01	2, 6
357	1.21	K6	−0.08	1, 3, 4	1653	1.21	K6e	−0.08	1, 3, 4
380	1.21	K4e	0.12	1, 4	1726	0.55	F7	0.00	6
430	0.81	G8	0.03	2	1776	0.72	G5	0.07	2, 6
451	1.21	K5e	0.02	1, 4	1883	1.03	K2	0.03	5
624	1.53	M2e	0.02	1	2016	1.22	K5e	0.00	1, 3
625	1.19	K0	0.34	6	2027	0.85	K0	0.00	2
659	0.94	G4	0.24	6	2034	0.96	K2.5e	−0.11	5
673	...	K6e	...	1, 3	2082	1.35	M0	...	1
676	1.30	K3.5e	0.28	1	2106	0.87	K0	0.02	2
686	1.39	K7e	0.02	3	2126	0.85	K0	0.00	2
738	1.17	G7	0.40	4, 6	2147	0.80	G9	0.00	2, 6
740	1.06	K3e	0.04	1	2193	1.37	K6e	0.08	1, 5
793	1.47	M0.5	0.01	3	2208	1.36	K6e	0.07	1, 4
799	1.34	K4	0.25	4, 6	2209	1.37	K6.5e	0.08	1
870	1.25	G4.5	0.53	6	2341	0.72	G4	0.02	6
882	1.07	K3	0.05	6	2548	1.33	K7e	−0.04	1, 4
885	1.02	K3	0.00	2	2588	1.18	K3e	0.16	1
890	1.33	M0e	−0.13	1	2601	1.53	M2e	0.02	1, 4
906	1.52	M3e	0.01	3, 5	2602	1.63	M2.5e	0.12	1
915	1.23	K6e	−0.06	1	2655	...	K4	...	4
945	...	K2	...	1	2881	0.97	K2	0.01	2
974	1.34	K7e	−0.03	1	2908	1.14	K4e	0.05	1, 4
1039	1.22	K1	0.32	5, 6	2927	1.26	K4e	0.17	1
1061	1.39	K5	0.20	4	2940	1.32	M0.5	−0.14	4
1081	1.42	K6e	0.13	1, 4	2966	1.50	M0	0.04	1, 4
1100	1.10	K3	0.08	2, 4, 5	3030	1.39	K7	0.02	4
1103	1.48	K7e	0.11	1	3187	1.16	K4.5e	0.07	1
1110	1.19	K6.5e	−0.10	1	3197	1.07	K3e	0.05	5
1124	0.98	K1	0.08	2, 6, 7	MT61	1.49	M3e	−0.02	3
1136	1.00	G8	0.22	2, 6					

REFERENCES.—(1) Kraft and Greenstein 1969; (2) Wilson 1966; (3) McCarthy and Treanor 1968; (4) Herbig 1962; (5) Haro, Chavira, and Gonzalez 1982; and (7) Zappala 1972.

Breger's claim that large reddenings are confined to a small region south of the Merope nebula. For HII 625 and HII 738 we derive reddenings essentially identical to Breger's values ($E(B-V) = 0.33$ and 0.39, respectively). The other rapid rotators in Table 5 have small reddenings consistent with the mean reddening to early-type stars in the cluster.

An additional check on the reddening estimates can be made with a color-magnitude diagram for the cluster; if the reddening vector is not parallel to the main-sequence slope, large reddenings should displace stars from the main-sequence locus. With the available photometry, the optimum diagram (largest difference between main-sequence slope and reddening vector) is I versus $B-V$. We present such a diagram in Figure 3. For simplicity, all stars are plotted in the diagram assuming $E(B-V) = 0.04$; stars for which we actually calculated $E(B-V) > 0.2$ are plotted twice, with the second point located at the position required by the estimated reddening. We have assumed a normal reddening law (Allen 1976), though there is some evidence this is not the case (Mendoza 1965). With the reddening correction, several of the heavily reddened stars go from more than 1.0 mag above the main sequence to within a few tenths of a magnitude of the main-sequence locus. The mean displacement above the main sequence for the heavily reddened stars changes from $\langle \Delta I \rangle = 0.64$ to $\langle \Delta I \rangle = -0.05$ after application of the reddening corrections. We believe this indicates that our reddening estimates are not greatly in error.

We conclude that a reddening correction corresponding to $E(B-V) = 0.04$ should be appropriate for most Pleiades stars, but that reddening corrections need to be calculated individually for stars near the line of sight to the molecular cloud foreground to the cluster. We agree with Breger (1985) that HII 625 and HII 738 are heavily reddened; application of the nominal reddening corrections make them the bluest late-type rapid rotators in the cluster. These reddening estimates should still be regarded as preliminary, however, because both stars are heavily spotted (thus causing their spectra and colors to be

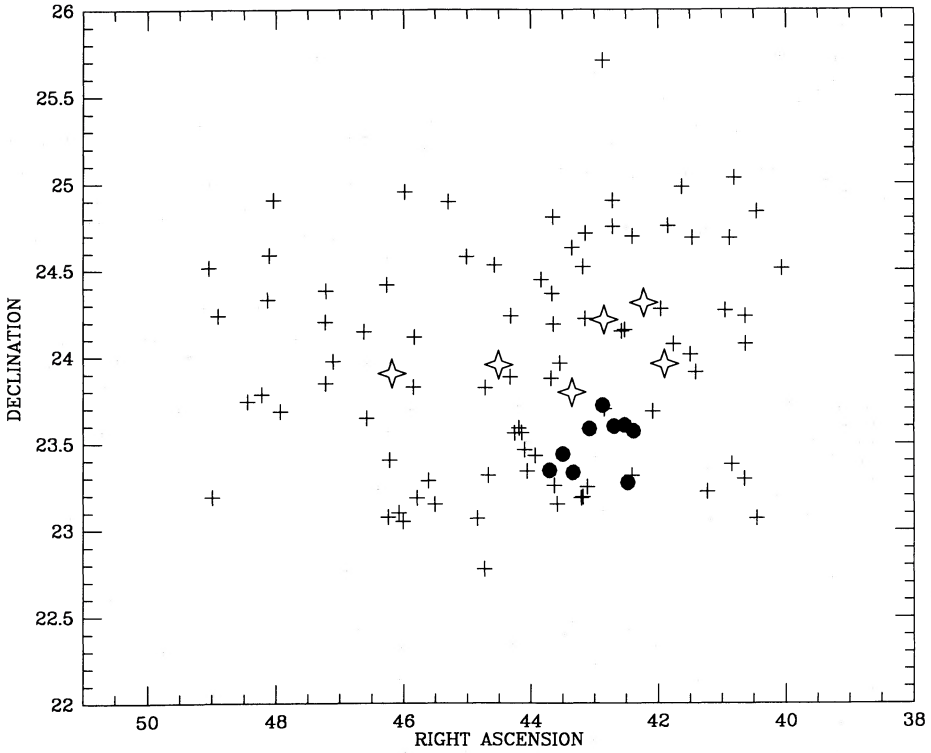

FIG. 2.—Location of Pleiades low-mass stars for which reddening estimates have been derived. For reference, the six brightest stars in the Pleiades are shown as well (*4-pointed stars*). Stars with $E(B-V) \leq 0.2$ are shown as plus signs; heavily reddened stars appear as filled circles.

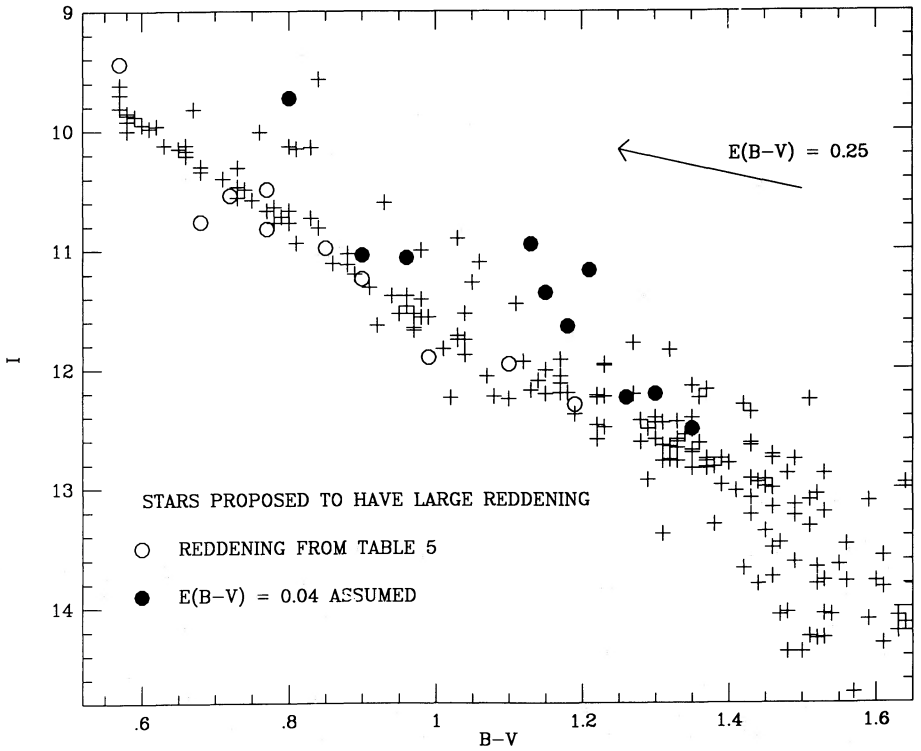

FIG. 3.—I vs. $B-V$ diagram for the Pleiades members with $BVRI$ photometry. The stars proposed to be heavily reddened are shown twice—as filled circles with $E(B-V) = 0.04$, and as open circles with reddening corrections from Table 5 or from Breger (1985). A reddening vector corresponding to $E(B-V) = 0.25$ is also shown.

peculiar) and because their observed colors may be somewhat inaccurate owing to the presence of reflection nebulae in the region.

IV. THE ROTATIONAL VELOCITY DISTRIBUTION

Studies of stellar rotational velocities can provide important information about the star formation process. Because high-mass stars do not have outer convective envelopes, it has long been assumed that their observed rotational velocity distribution closely resembles their initial angular momentum distribution (Kraft 1967). Earlier than about F0, the rotational velocity distribution in a given spectral type range (or mass) can generally be fitted well by a Maxwell-Boltzmann distribution with a small excess of slow rotators (Dworetsky 1974; Conti and Ebbets 1977; Wolff, Edwards, and Preston 1982). Possible explanations for this form for the distribution are provided in Wolff, Edwards, and Preston. The variation of the rotational velocity properties with mass are also of interest. For high-mass stars, Kraft (1970) showed that the mean angular momentum per unit mass follows a power-law relation such that $J/M = KM^{0.57}$. Stars later than about F2 do not follow that law, presumably because of analogs of the solar wind carrying away angular momentum. Among F dwarfs older than the Pleiades, there is a slow decrease of the mean rotational velocities with time (Kraft 1967; Skumanich 1972; Soderblom 1983), supporting the idea of angular momentum loss via a wind. Stars later than G0 in the Pleiades or other young clusters are generally too faint for photographic, high-resolution spectroscopy. Hence, prior to 1980, essentially no observational data existed to constrain models of the angular momentum evolution of young, low-mass stars. In SHSB and SHBJ we provided spectroscopic evidence that many low-mass stars arrive on the main sequence with quite large rotational velocities ($v \sin i$ up to 150 km s^{-1}). If solid-body rotation is assumed, the most rapidly rotating G and K stars in the Pleiades and α Per clusters have angular momenta consistent with Kraft's power-law relation for high-mass stars. Even in these young clusters, the rapid rotators are in the minority, however; more than half of the late-type stars have rotational velocities at or below our resolution limit of about 10 km s^{-1}. By observing a more complete sample of stars in the Pleiades and other young clusters, we hope to determine the cause for this range in rotational velocities and use our data to help model the star formation process in open clusters.

a) Location of Rapid Rotators in an H-R Diagram

In SHSB we provided a V versus $V-I$ diagram showing the location of the rapid rotators identified at that time relative to other stars in the cluster. No obvious differences were present, indicating neither that the rapid rotators were more (or less) often binaries than slow rotators nor that the K dwarf rapid rotators were so young as to be still pre–main-sequence objects. The larger data set now available, plus the new reddening corrections for stars near the Merope nebula, allow a more quantitative comparison. Figure 4 shows a color-magnitude diagram for the Pleiades stars, with different rotational velocity ranges indicated by different symbols. A reddening correction appropriate for $E(B-V) = 0.04$ assum-

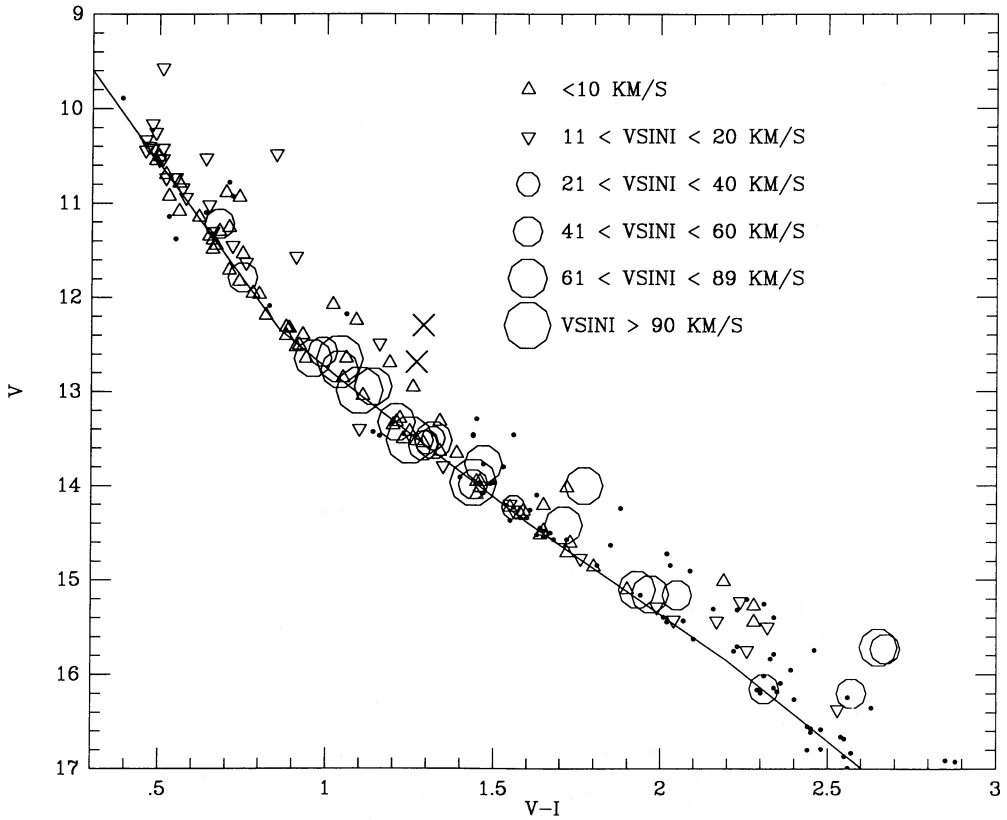

FIG. 4.—Reddening-corrected V vs. $V-I$ diagram for late-type stars in the Pleiades. The solid line is a fit to the lower envelope to the distribution; it is not the ZAMS. HII 625 and HII 738 are plotted twice, as crosses for $E(V-I) = 0.065$ and as large circles when the reddenings from Table 5 are used. With the larger reddenings, these two stars become the bluest rapidly rotating late-type dwarfs in the cluster.

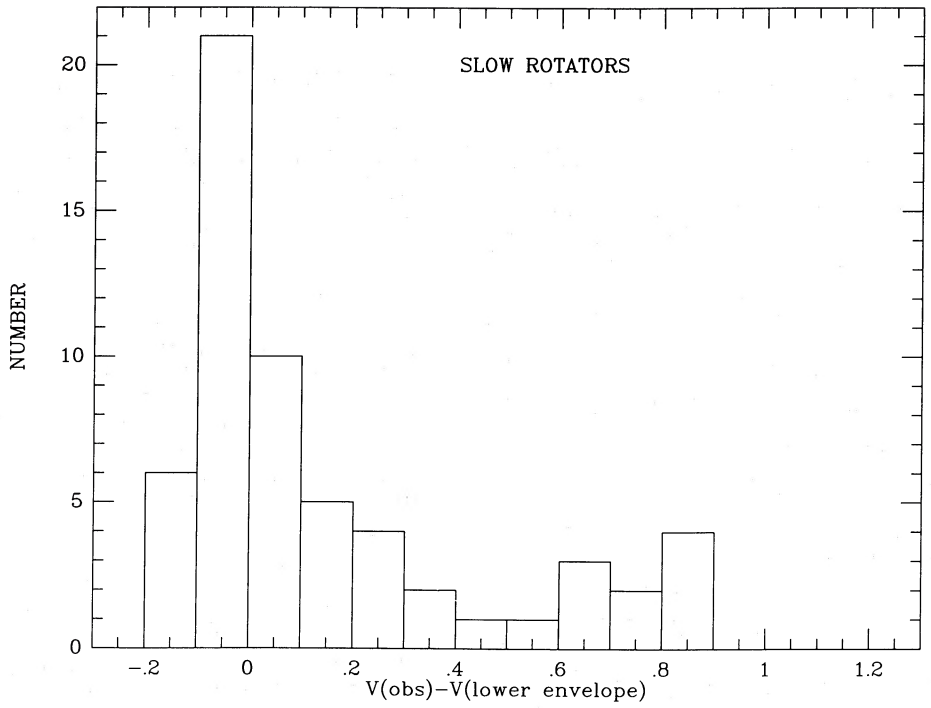

FIG. 5*a*

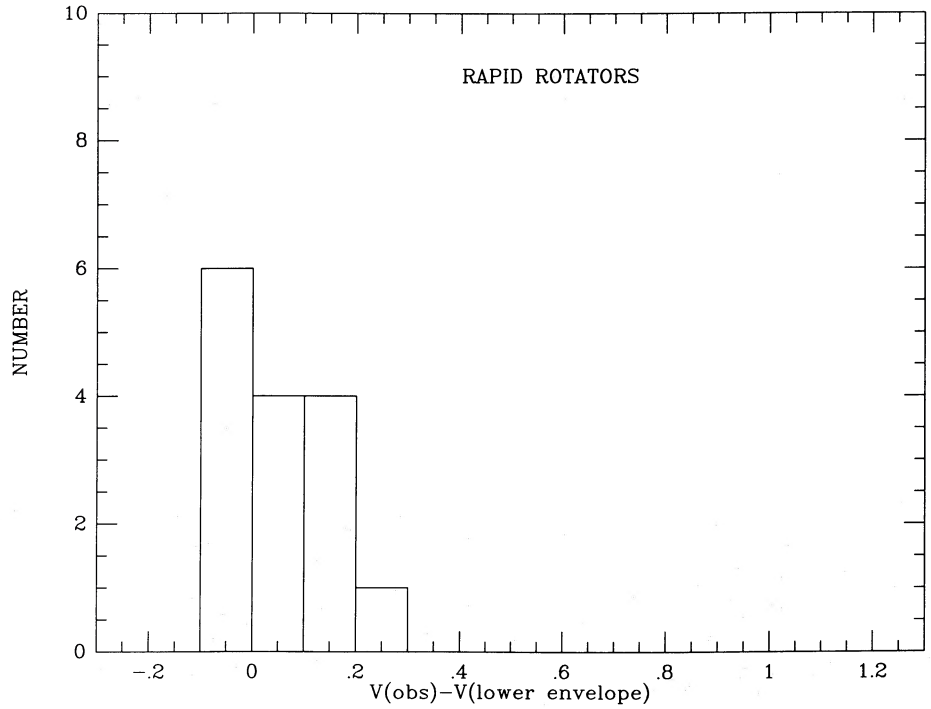

FIG. 5*b*

FIG. 5.—Histogram of the vertical displacement of (*a*) slow and (*b*) rapid rotators relative to the solid line in Fig. 4 for the color range $0.6 < V-I < 1.5$. The comparison indicates that the rapid rotators include fewer photometric binaries.

ing a standard reddening law has been applied, except for the stars with $E(B-V) > 0.20$, where the larger corrections were used.

Figure 4 shows some differences between the rapid rotators and the slow rotators, particularly for $V-I < 1.5$. In order to obtain a quantitative measure of the location of the rapid rotators in this diagram, we have fitted a curve to the lower envelope of the observed distribution, and then determined the displacement of all stars in the diagram relative to this curve. Histograms of these displacements for slow rotators ($v \sin i < 20$ km s^{-1}) and rapid rotators for $0.6 < (V-I)_0 < 1.50$ are provided in Figure 5. The rapid rotators are less often displaced above the single-star main sequence, presumably indicating that slow rotators are more likely to be binaries. This differs from conclusions reached in SHSB, primarily because of the shift in position of HII 625 and HII 738 resulting from the large reddening corrections that we now estimate. An obvious possible interpretation of the new result is that late-type binary stars deposit much of the initial angular momentum in orbital motions, and thus have smaller rotational velocities. However, since the orbital angular momentum of a typical binary is much greater than the rotational angular momentum of even the most rapidly rotating stars in our sample, it is not clear that duplicity should exclude rapid rotation.

For the stars redder than $V-I = 1.5$, the slow and rapid rotators have similar distributions in Figure 4. Because our survey is essentially magnitude-limited, however, we have not yet obtained spectra for many stars near the lower envelope to the distribution in this color range. Additional spectra are needed in order to perform the test adequately.

b) *Variation of Rotational Velocity with Mass*

There are two factors which might cause the rotational velocity distribution for low-mass stars to be a function of mass. First, pre–main-sequence contraction time scales increase for lower mass stars, so that solar-type stars with the nominal cluster age (7×10^7 yr) should have arrived on the main sequence 40 million years ago, while M dwarfs should still be contracting to the main sequence. Second, the thickness of the outer convective envelope also increases to lower mass stars, with less than 10% of the moment of inertia of a 1 $M_\odot$ star in the convective envelope to 100% of the star being convective for a 0.3 $M_\odot$ star. Because it is probably just the outer convective envelope that is initially spun down by the wind (Endal and Sofia 1981), we expect longer spin-down time scales for lower mass stars if angular momentum loss rates do not significantly increase for lower mass stars.

We do not directly measure mass, of course, so we have chosen to use the star's $V-I$ color as the mass surrogate. Figure 6 shows the distribution of observed $v \sin i$ versus $V-I$. As with the other figures, $E(V-I) = 0.07$ is assumed; for HII 625 and HII 738 a second symbol shows their location after correction for their larger reddenings. A similar diagram, but with fewer points, was shown in SHBJ. The salient features of the diagram are the following: (1) The G stars in the cluster ($0.44 < V-I < 0.72$) are essentially all slow rotators, with $v \sin i < 20$ km s^{-1}. If the large reddening corrections for

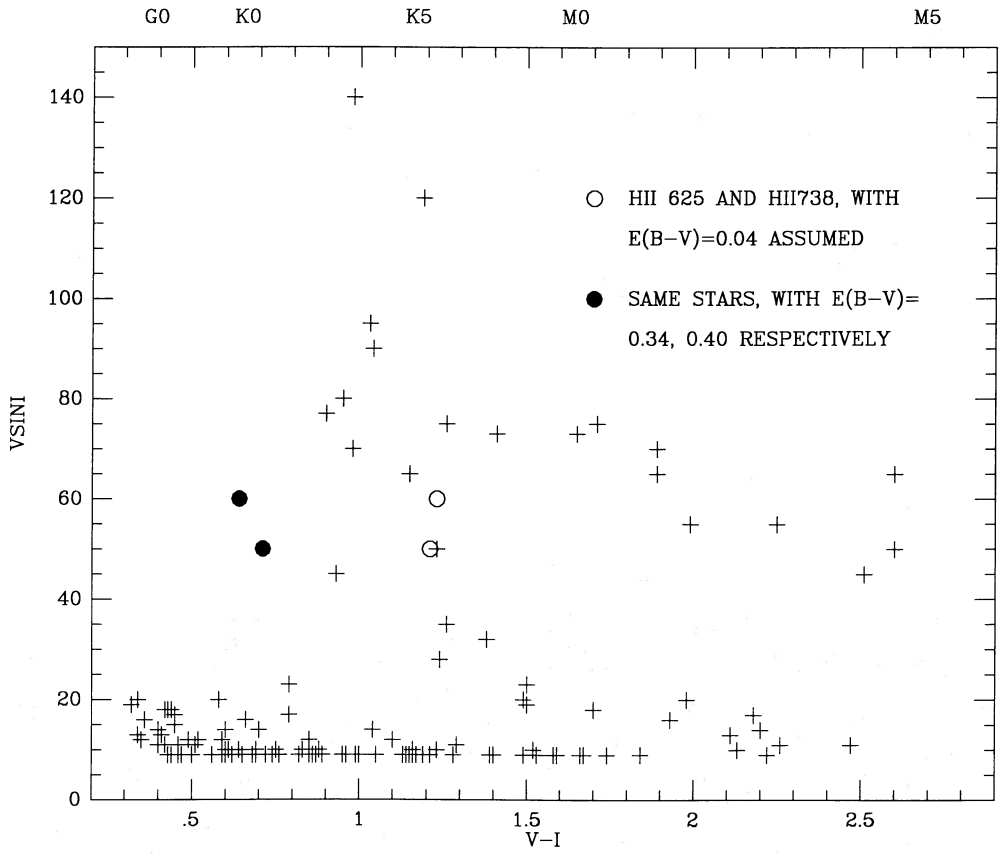

FIG. 6.—Distribution of spectroscopic rotational velocities as a function of reddening-corrected $V-I$ color for the Pleiades. HII 625 and HII 738 are shown twice, corresponding to the two alternative reddening corrections.

HII 625 and HII 738 were not incorporated in the diagram, the red limit to the slow rotation zone would be $V-I = 0.96$. (2) There is an upper envelope to the projected rotational velocities which slopes to smaller maximum rotational velocities for redder stars. The most rapidly rotating K dwarf has $v \sin i \approx 140$ km s^{-1}, while the most rapidly rotating late-type M dwarf has $v \sin i \approx 60$ km s^{-1}. (3) Even in the region where rapid rotation is common, at least half of the stars have projected rotational velocities near (or less than) 10 km s^{-1}. The rotational velocity distribution is somewhat bimodal, with very few stars at a given color having projected rotational velocities in the range $20 < v \sin i < 50$ km s^{-1}.

It might be argued that point 3 simply reflects the influence of sin i, and that a distribution of equatorial velocities with few slow rotators combined with a reasonable distribution of inclination angles could reproduce the observed distribution. We do not believe that is the case, since a random distribution of axes strongly favors $\sin i \approx 1$. Also, among the K dwarfs, the stars with large $v \sin i$ have Hα in emission, while those with $v \sin i < 15$ km s^{-1} have Hα in absorption. This is as expected given a rotation-activity correlation if the stars with small $v \sin i$ are intrinsically slow rotators and not nearly pole-on rapid rotators. Finally, among high-mass stars in the Pleiades, the distribution of projected rotational velocities (Fig. 7) does not show a peak at low $v \sin i$.

Conceivably, other selection effects or physical processes might affect our observed rotational velocity distribution and alter our interpretation. For instance, it might be argued that we are significantly biased toward inclusion of rapid rotators, because we have preferentially observed short-period variables and heavily spotted stars. That bias is present; however, in the color range where photometric programs have provided such information, we are more than 90% complete for Pleiades members in Hertzsprung's catalog. Thus, the bias cannot affect the calculated distribution greatly. Similarly, it is possible that our selection procedure biases us toward inclusion of rapid rotators among the reddest stars in Figure 6. That might occur because the stars redder than $V-I \approx 1.6$ were generally discovered in flare star surveys for Pleiades members. If a significant number of nonflaring, late-type Pleiades members exist, and if flare activity is connected with rotation, our sample could be biased. Because we see no connection between rotation and Hα emission in this color range (Fig. 1), a significant bias is unlikely. Also, we have searched for previously unidentified, late-type members of the cluster via a blink survey for faint red stars with follow-up low-dispersion spectroscopy. Only two new possible cluster members were found in a region containing 10 flare star cluster members. Finally, our interpretation would be in error if many of the rapid rotators gained their large rotational velocities from exchange of orbital for rotational angular momentum in a close binary, as is assumed to be the explanation for RS CVn stars. The quite large fraction of late-type stars that are rapid rotators in these clusters make that hypothesis unlikely. Additionally, the dispersion of the radial velocities for the rapid rotators relative to the mean cluster velocity is small and consistent with our measurement errors; we also see no evidence of radial velocity variability for the rapid rotators.

c) *Rotation and X-Ray Activity*

X-ray observations of the Pleiades cluster were obtained with the *Einstein Observatory*, and the results of that survey have recently been published (Caillault and Helfand 1985). Most of the K and M dwarfs in the cluster have quiescent X-ray levels below the detection limit of the survey, which hampered the analysis. However, after consideration of the X-ray data and the published rotational velocity information, Caillault and Helfand concluded that there is "no evident correlation between rotation and X-ray emission" among the late-type dwarfs (K0–M3) in the Pleiades. In fact, when one

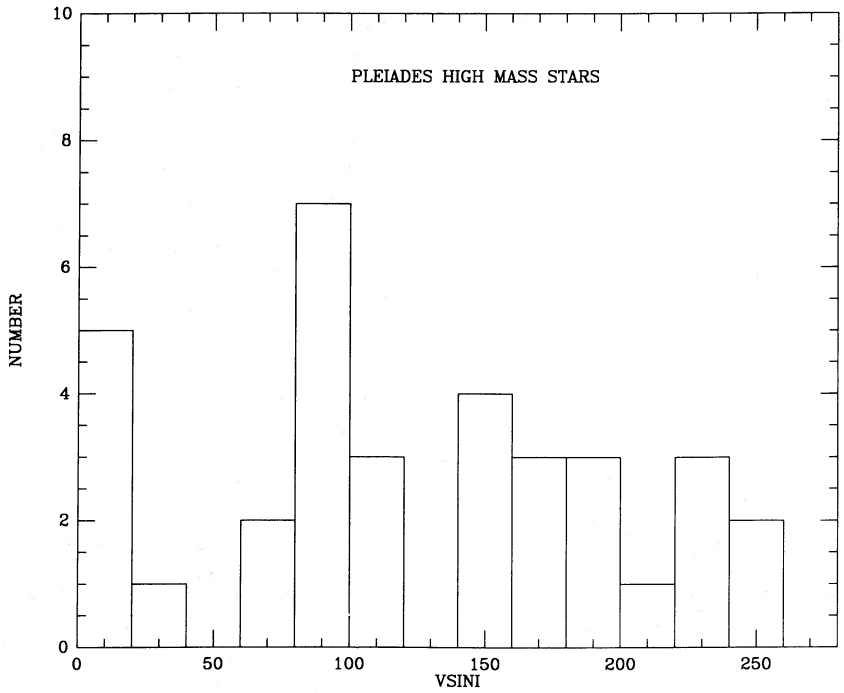

FIG. 7.—Histogram of the spectroscopic rotational velocities for high-mass stars in the Pleiades (Kraft 1967)

considers the new rotational velocity data and deletes rotational velocities inferred from incorrect periods for five of the stars reported by Meys, Alphenaar, and van Leeuwen (1982) (see SHSB and van Leeuwen, Alphenaar, and Brand 1986), there is a good correlation between rotation and X-ray emission.

To illustrate this correlation, we examine the statistics of rotation and X-ray detection among stars with $0.9 < V-I < 1.3$, the color range where the most rapidly rotating K dwarfs are found and where we have a fairly complete sample of rotational velocities. Table 6 shows the stars for which we have photometry in this color range, as well as the X-ray and rotational velocity data. Seven of the 10 X-ray–detected stars are rapid rotators, with $v \sin i > 40$ km s^{-1}. Only one of the 14 stars with $v \sin i < 15$ km s^{-1} is detected in the X-ray survey; we do not have rotational velocity data for the two remaining X-ray detections. Thus, X-ray emission and rotation are closely related, in that the mean X-ray luminosity for the rapid rotators is greater than that for slow rotators of the same color. The correlation is not perfect, however; four rapid rotators in this color range were not detected in the X-ray survey, including the two most rapidly rotating stars. A correct summary of the X-ray observations for K and M dwarfs in the Pleiades is that there is a correlation between rotation and X-ray emission, consistent with Walter's (1982) exponential decay relation, which predicts a steep relation between rotation and X-ray emission for low rotational velocities and a relatively flat relation for large rotations.

TABLE 6

X-RAY DATA FOR STARS WITH $0.9 < V-I < 1.3$[a]

Star	log L_x	$v \sin i$
HII 97	<	<
HII 324	30.03	90
HII 380	...	<
HII 451	<	<
HII 559	30.03	65
HII 625	29.84	50
HII 636	<	<
HII 659	29.77	...
HII 738	29.81	60
HII 740	...	14
HII 879	<	<
HII 882	<	80
HII 883	<	<
HII 885	<	<
HII 1039	29.62	10
HII 1100	<	<
HII 1110	...	10
HII 1136	31.25	...
HII 1305	<	120
HII 1332	<	<
HII 1454	<	<
HII 1512	...	<
HII 1531	29.68	50
HII 1553	...	12
HII 1883	<	140
HII 2016	...	10
HII 2034	29.54	77
HII 2244	29.66	45
HII 2588	<	<
HII 2741	<	10
HII 2870	<	<
HII 2881	<	12
HII 2908	...	...
HII 3019	...	<
HII 3163	<	70
HII 3187	...	...
HII 3197	...	...
T 166	...	...

[a] Stars with $v \sin i < 10$ km s^{-1} or with X-ray upper limits are indicated by <; stars with no $v \sin i$ or X-ray data are denoted by an ellipsis.

As a curiosity, we note that the three X-ray detections in this color range that are not known to be rapid rotators are all heavily reddened according to Breger (1985) or our discussion in § II. One of these stars, HII 1136, is the "superflare" star reported by Caillault and Helfand (1985). We do not have echelle spectra for HII 659 or HII 1136 because without large reddening corrections they lie well above the Pleiades single-star main sequence, and we considered them to be possible nonmembers. With the proposed reddening corrections, they fall quite near the main sequence, and we no longer have any reason to believe they might not be Pleiades members. Because the molecular cloud is thought to be passing through the cluster, we have considered mechanisms which might link the X-ray activity of these stars with their location near the cloud. We considered whether accretion from the cloud could account for the observed X-ray emission. Although estimates using the Bondi-Hoyle cross section suggest that this mechanism could produce the required luminosity, any modest stellar wind would prevent accretion, and the X-ray luminosity resulting from the interaction of the rapidly moving wind with the cloud is small. We conclude that there is no physical reason to expect a connection between X-ray emission and location in or behind the CO cloud, and attribute the apparent correlation to a statistical fluctuation.

V. A MODEL FOR THE ROTATIONAL VELOCITY EVOLUTION OF LOW-MASS STARS

The rotational velocity evolution of low-mass stars is of great interest for its implications concerning angular momentum loss and internal differential rotation. Stellar spin-down (or spin-up) also has some bearing on the origin of the range in stellar rotational velocities in the Pleiades sample. The large spike in the $v \sin i$ distribution at low velocities among the K and M dwarfs is particularly intriguing. It may imply a very large age spread in the Pleiades, giving the oldest stars enough time to spin down (MDC; SHSB). Alternatively, there may have been an initial population of extremely slowly rotating stars (SHSB). Or angular momentum loss may not be a simple function of rotational velocity. Sorting out these possibilities clearly requires an understanding of the evolution of rotation between the time a star forms and its main-sequence phase.

The evolution of stellar rotation depends upon the rate of angular momentum loss and the transport of angular momentum in stellar interiors. Wind theory for pre–main-sequence stars cannot be used to predict mass-loss rates (Hartmann 1985), and angular momentum loss due to the coupling of the wind with the stellar magnetic field depends sensitively on the magnetic field strength and geometry, which are also unknown parameters (Mestel 1984). Even the internal transport of angular momentum is not very well understood (Endal and Sofia 1981). In this situation one must rely heavily on observations to indicate the level of angular momentum loss.

Previous observations indicated that surface rotational velocities of solar mass stars decay as $v \sim t^{-1/2}$ between the age of the Pleiades and the age of the Sun (Soderblom 1983). However, there is no *a priori* reason to assume that this relation can be extended to earlier ages. Indeed, the rapid spin-

down of G stars indicated by the α Per–Pleiades comparison shows that the Skumanich relation does not hold in this case.

Rotational velocity measurements are now available for a number of low-mass T Tauri stars (HHSM; Bouvier *et al* 1986), so that we may begin to investigate the evolution of low-mass stellar rotation starting from early pre–main-sequence phases. In what follows we shall take the T Tauri data as a starting point to quantify rotational evolution and its implications for angular momentum loss.

a) Rotational Evolution in the Absence of Angular Momentum Loss

Because T Tauri stars are known to have low rotational velocities (Vogel and Kuhi 1981; HHSM; Bouvier *et al.* 1986), the observations of young cluster objects imply that low-mass stars must spin up as they contract to the main sequence. HHSM attempted to estimate the main-sequence rotational velocities implied by their observations of low-mass T Tauri rotation, assuming that no angular momentum loss occurs. A version of their results is shown in Figure 8 for stars in the mass range 0.5–1.0 $M_{\odot}$. (The original results were put into 20 s^{-1} bins, and we have divided the contents evenly into 10 km s^{-1} bins for convenience in comparing with the cluster data.) The assumptions involved in producing this distribution are as follows: (1) The luminosities and effective temperatures derived by Cohen and Kuhi (1979) for T Tauri stars are correct. (2) Standard evolutionary tracks can be used to assign masses to T Tauri stars (cf. Cohen and Kuhi 1979). (3) Upper limits for the original T Tauri v sin i's were incorporated to produce a "best estimate" of the true v sin i distribution using the Kaplan-Meier maximum-likelihood estimator (cf. HHSM). (4) The T Tauri stars are assumed to contract to the main sequence without any angular momentum loss, and are assumed to rotate as solid bodies. (5) The sample is representative of T Tauri stars. Concerning the last point, we note that strong-emission T Tauri stars were not included in the HHSM sample because of the absence of photospheric lines near 5200 Å. This does not lead to a strong bias in our main-sequence rotational velocity distribution because the strong-emission objects are a relatively small subset of the total observed sample. Subsequent observations (Hartmann and Kenyon 1986) of a few of the strong emission line stars at longer wavelengths suggest that their rotational velocities are not very different from those characteristic of the larger sample. The most troubling of these assumptions is the first one. T Tauri stars often exhibit obviously peculiar spectra; assigning accurate spectral types is often difficult; and in many cases, extinction corrections are large. Few observational tests of the theoretical evolutionary tracks exist. Lacking any alternative, we proceed cautiously with the interpretation of the distribution shown in Figure 8; the reader should keep in mind the fundamental uncertainties involved.

Because Figure 8 assumes no angular momentum loss subsequent to the T Tauri phase, it should serve as an upper limit (in some sense) to the rotational velocity distribution in young open clusters if the above assumptions are valid and if the T Tauri stars and open cluster stars have approximately the same initial angular momentum distributions. As a consistency check, we present the Pleiades rotational velocity distribution divided into two color or mass bins in Figure 9. It is encouraging to find that the v sin i distribution resulting from projecting T Tauri rotation to the main sequence permits some angular momentum loss. Clearly rapid rotators can result, adopting standard evolutionary tracks, as long as angular momentum loss during contraction to the main sequence is not too large.

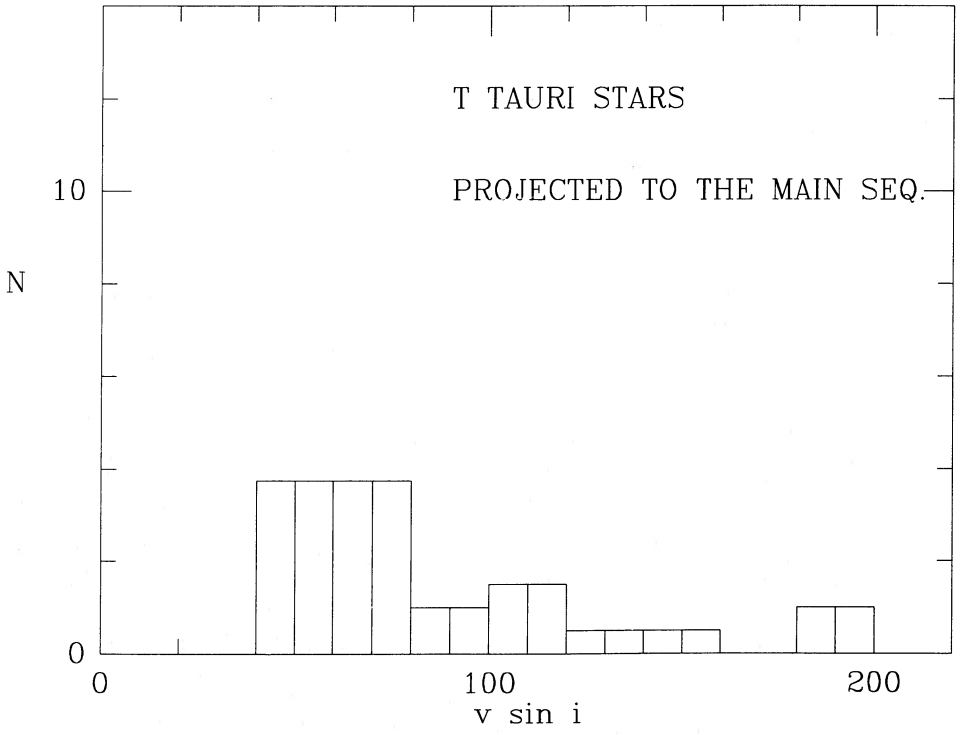

FIG. 8.—Model rotational velocity distribution on the main sequence for low-mass stars derived from the observed rotational velocity distribution for T Tauri stars (Hartmann *et al.* 1986), assuming no angular momentum loss during subsequent pre–main-sequence evolution. See § V*a* for further discussion.

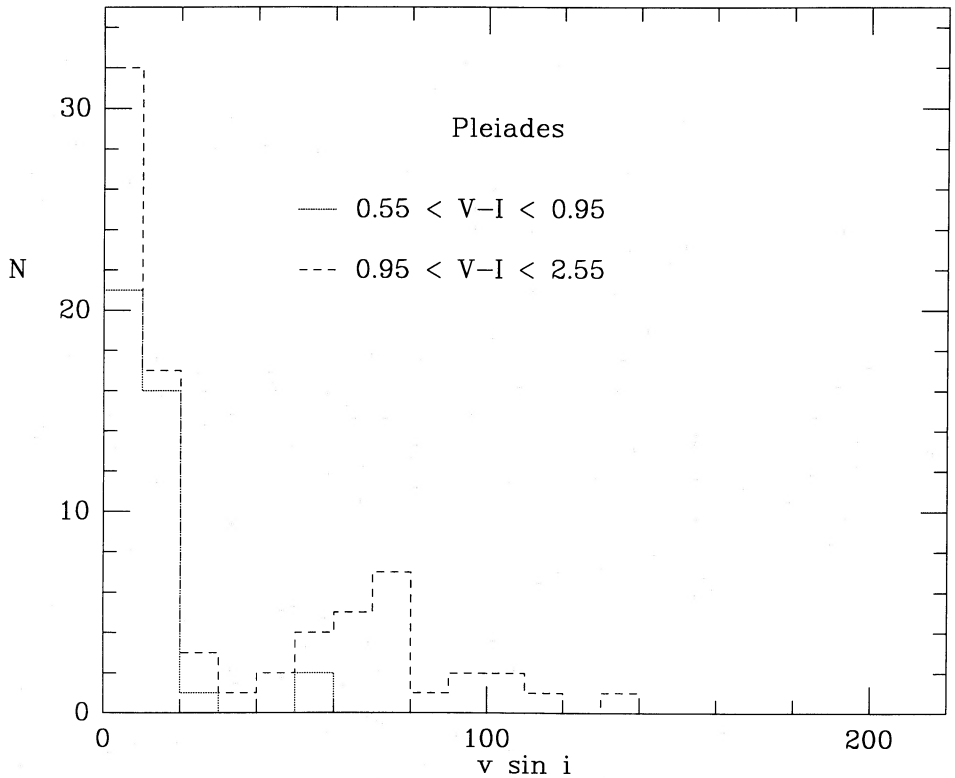

FIG. 9.—Rotational velocity histogram for G2–K1 and K2–M4 dwarfs in the Pleiades. HII 625 and HII 738 are included in the former group, on the assumption that the large reddening corrections are accurate.

It should be noted that the projected rotational velocity distribution shown in Figure 8 is uncertain at the smallest values of $v \sin i$ because of the presence of upper limits in the original data. The Kaplan-Meier estimator does not redistribute upper limits into bins below the last bin containing a detection (cf. HHSM). Thus, some of the stars shown in the 40–80 km s^{-1} range might actually reside in bins <40 km s^{-1}. Direct measurements of the rotational periods for two of the T Tauri stars with upper limits to $v \sin i$ suggest that the true equatorial velocities are not much below the upper limit value (cf. Rydgren *et al.* 1985; Vrba *et al.* 1984), but the result is obviously uncertain.

b) *Angular Momentum Loss*

Models have been constructed for the rotational evolution of a solar mass star (cf. Endal and Sofia 1981) in which various assumptions are made about the angular momentum loss rate and the internal diffusion of angular momentum. Because of the uncertainties involved in these mechanisms for angular momentum transport, a large range of parameter space must be considered. We make an initial attack on this problem from a different direction. We consider schemes for *surface spin-down* which will transform the rotational velocity distribution shown in Figure 8 into something like the Pleiades distributions shown in Figure 9. As the transport of angular momentum in stellar interiors is better understood, possibly in conjunction with stellar oscillation measurements revealing the internal differential rotation of stars, it will be possible to infer more realistically the amount of total angular momentum loss required by the observation of surface spin-down. In turn, this may ultimately constrain theories of mass loss and large-scale magnetic field structure.

The usual Skumanich (1972) relation between rotational velocity v and age t for main-sequence solar-type stars (in the limit of large t) is

$$\frac{v}{v_0} = \left(\frac{t}{t_0}\right)^{-1/2} . \tag{1}$$

This relation implies that the rate of decay of rotational velocity $dv/dt \sim -v^3$. The relationship between the initial rotational velocity v_i and the final rotational velocity v_f of a star is then

$$\frac{1}{v_f^2} - \frac{1}{v_i^2} = \frac{\Delta t}{v_0^2 t_0} , \tag{2}$$

where Δt is the elapsed time interval.

We have applied various forms of this relation to the distribution shown in Figure 8. Given the uncertainties in the initial distribution, we treat the horizontal axis as the equatorial velocity v(eq), neglecting the $\sin i$ dependence of the sample. As indicated by one result shown in Figure 10, the distributions produced by this spin-down formula never look much like the Pleiades distribution for K and M stars. The reason is that this dependence of spin-down compresses the range of $v \sin i$ as time goes on, because the rapidly rotating stars spin down much faster than the slowly rotating stars. Equation (2) produces distributions which have a narrower range of rotational velocity than that observed in the Pleiades. Therefore, it is unlikely that a Skumanich law braking mechanism is appropriate for the rapidly rotating K and M dwarfs. However, this braking law cannot be completely excluded by our observations because of uncertainties due to placing T Tauri stars in the H-R diagram, upper limits in the rotational velocity data, and the possibility of noncoeval star formation.

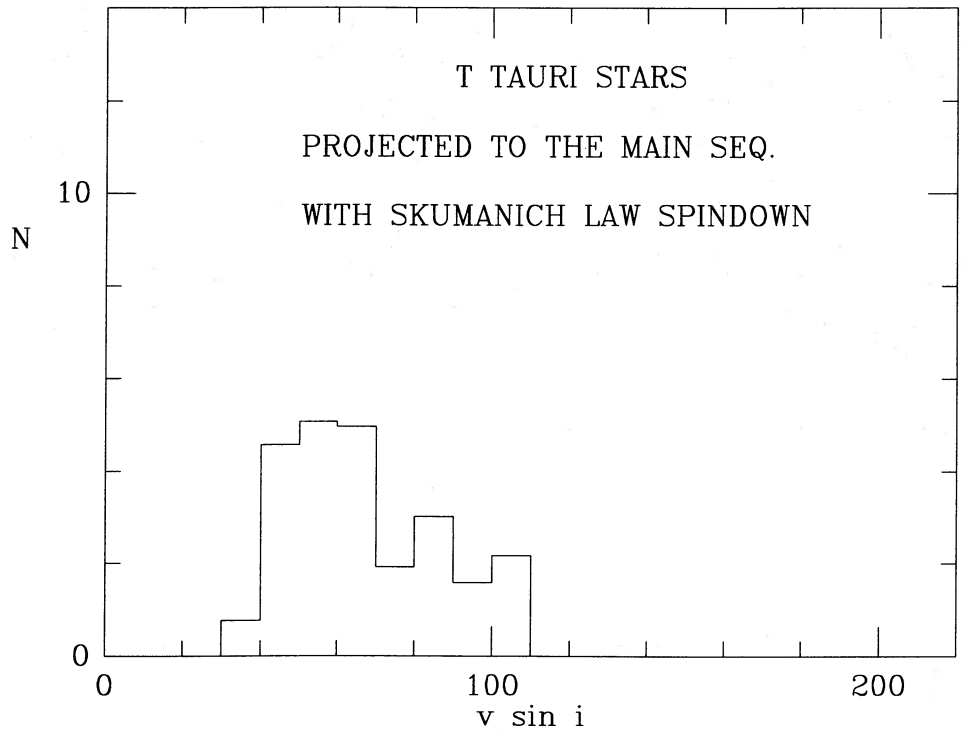

FIG. 10.—Rotational velocity distribution for low-mass stars of Pleiades age, assuming the distribution shown in Fig. 8 as input and a Skumanich law decay of rotational velocity with time.

We next considered a qualitatively different braking law for which the angular momentum loss rate is completely independent of rotational velocity. This can hold only to some point, since there is observational evidence for the Skumanich law for older stars (Soderblom 1983). Thus, we assume that the angular momentum loss rate is constant until the star reaches a rotational velocity of 10 km s^{-1}, at which point the braking is assumed to occur on a much longer time scale consistent with the Skumanich relation. In particular, we assume

$$\begin{aligned} dv/dt &= \text{constant}\,, \quad v > 10 \text{ km s}^{-1}\,, \\ dv/dt &\sim 0\,, \qquad\quad v \leq 10 \text{ km s}^{-1}\,. \end{aligned} \tag{3}$$

The details of braking at rotational velocities below $v = 10$ km s^{-1} do not concern us greatly, since this coincides with our upper limits. The total rotational braking $\Delta v = (dv/dt)\Delta t$ over a time scale Δt is then

$$\begin{aligned} v_f &= v_i - \Delta v\,, \quad \Delta v < v_i - 10 \text{ km s}^{-1}\,, \\ v_f &= 10 \text{ km s}^{-1}\,, \quad \Delta v > v_i - 10 \text{ km s}^{-1}\,. \end{aligned} \tag{4}$$

Some results using this braking scheme are shown in Figure 11. The distribution is remarkably similar to the observed v sin i distribution for K and M stars in the Pleiades. Because the angular momentum loss is independent of rotation above 10 km s^{-1}, the slow rotators collect at the left end of the figure, producing a low-velocity spike in the distribution.

Is there any reason to propose an angular momentum loss rate that is independent (or relatively independent) of rotation rate for rapidly rotating stars? Although we cannot measure mass-loss rates or magnetic fields directly in these stars, one might look to chromospheric and coronal emission as tracers of magnetic activity. Observations of Ca II fluxes suggest that chromospheric emission is not a strong function of rotation in very young main-sequence stars (Hartmann *et al.* 1984). We have obtained MMT spectra of rapid and slowly rotating Pleiades and α Per stars, which show very modest differences in chromospheric emission for stars ranging in v sin i from 10 to 100 km s^{-1}. This does not seem to be a property of the changing atmospheric temperature structure. Walter (1982) showed that the X-ray emission from late-type stars is best fitted by an exponential relation of the form $L_x/L_{\rm bol} \propto e^{-0.16/\Omega}$. This relation leads to only a weak correlation between X-ray luminosity and rotation for rotational velocities greater than 30 km s^{-1}. As noted in § IV, the Pleiades X-ray data (Caillault and Helfand 1985) are consistent with this relation. This situation stands in marked contrast with the results for the relatively slowly rotating stars of Hyades age or older, in which L_x or $L_{\rm Ca\,K} \propto \Omega^n$, with n in the range 1–2 (Skumanich 1972; Pallavicini *et al.* 1981; Noyes *et al.* 1984; Hartmann *et al.* 1984). Thus, the observable manifestations of magnetic activity and coronal heating for rapidly rotating stars do not scale with rotation in the same way as for slowly rotating stars. This suggests that the angular momentum loss rate, which is controlled by magnetic field strength and coronal mass loss, may not be a strong function of rotation for rapidly rotating stars.

It is possible to explain the distribution of rotational velocities we observe with a model where the angular momentum loss rate is strongly coupled to the star's angular rotational velocity if there is a relatively large age spread among the low-mass stars in the Pleiades. We have now shown that invoking angular momentum loss that is relatively independent of rotation for v(eq) > 10 km s^{-1} enables us to produce a distribution of rotational velocities that matches the Pleiades reasonably well without invoking an age spread. Although it has been suggested that a large age spread might be present among the low-mass stars in the Pleiades (Herbig 1962; SHSB;

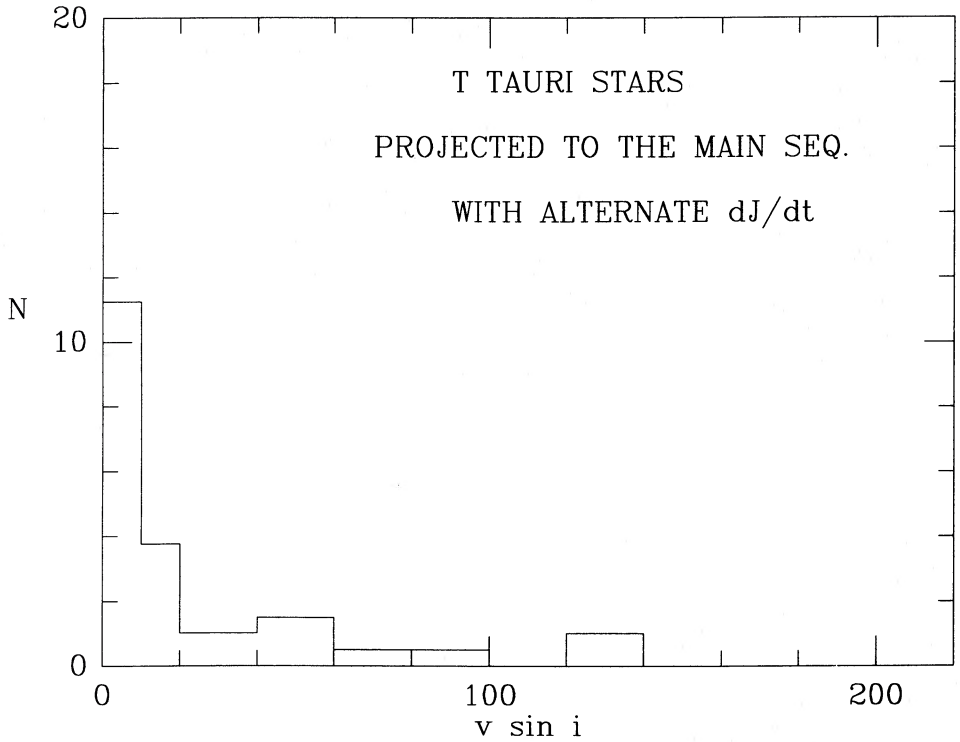

FIG. 11.—Same as Fig. 10, but with an assumed angular momentum loss rate that is independent of rotational velocity for $v_{rot} > 10$ km s^{-1}. We have normalized this distribution so that it corresponds to stars with mass near 0.7 $M_\odot$ or $V-I \approx 1.0$.

Duncan and Jones 1983), constructing a theoretical model of a star-forming region with such an age spread is a formidable challenge. Given a Skumanich spin-down law, the presence of a significant fraction of slow rotators among the K and M dwarfs would seem to require an age spread comparable to the present age of the Pleiades. The crossing time for the present-day Pleiades cluster is about 3×10^6 yr (for a cluster radius of 2 pc and a velocity dispersion of 0.7 km s^{-1}); the sound travel time across the protocluster is not very different from that. The formation of a number of stars would presumably serve to heat surrounding gas and set it in motion, either via the ultraviolet radiation fields of high-mass stars or via the winds and jets that are common for low-mass stars during the early stages of their pre–main-sequence evolution. With such a short dynamical time scale, it is hard to see how much gas will remain in the cluster for 10^8 yr after star formation begins in earnest, in order to form a significant fraction of the star cluster over this spread in time (but see Norman and Silk 1980, who hypothesize that low-mass star formation could input just enough energy to the protocluster to support the cloud).

We next consider the dependence of rotation on spectral type observed in the Pleiades. Originally we suggested that G dwarfs have spun down prior to lower mass starts in the Pleiades because they arrived first on the main sequence (at $\tau \sim 3 \times 10^7$ yr), while the K dwarfs are still contracting (SHSB). However, it seems unlikely that this effect alone can account for the rapid change in rotation occurring at around $V-I = 1.0$. The reason is that K dwarfs do not contract substantially between the ages of 3×10^7 and 7×10^7 yr, according to standard evolutionary calculations (VandenBerg 1986, private communication). H-R diagrams for the Pleiades, α Per, and IC 2391 clusters confirm that K dwarfs are only slightly above the main sequence at 3×10^7 yr and on the main sequence by 7×10^7 yr (Stauffer 1984; SHBJ; Stauffer *et al.* 1986). Something else must account for the difference in rotational velocity distribution between the G and K dwarfs.

One solution is simply that spin-down is much more efficient in G dwarfs than in K dwarfs. Given our ignorance of the processes responsible for magnetic field generation and mass ejection, we cannot exclude such a possibility. Nevertheless, this solution is somewhat unsatisfying.

An alternative explanation, as suggested in Paper I and SHBJ, is that only the convective envelope of the star is spun down at first. Therefore, because G dwarfs have smaller convective zones than K dwarfs, for the same angular momentum loss the G dwarf *surfaces* will spin down first.

We explore this possibility in the context of our simplified investigation of angular momentum loss. We write the equation for conservation of angular momentum as

$$I\omega_f = I\omega_0 - \Delta J \,, \tag{5}$$

where I is the moment of inertia of the material being spun down, ΔJ is the angular momentum lost, ω is the angular velocity, and subscripts f and 0 refer to the final and initial states, respectively. This equation assumes that the spinning object is in solid-body rotation. Rearranging terms, we can write this result in terms of the surface equatorial velocity $v(\mathrm{eq}) = R\omega$,

$$v(\mathrm{eq})_f = v(\mathrm{eq})_0 - (\Delta J)R/I \,. \tag{6}$$

We recover our previous results (eq. [4]) if we assume that $(\Delta J)R/I$ is independent of rotation and mass in the range 0.5–1.0 $M_\odot$ [except below $v(\mathrm{eq})_f = 10$ km s^{-1}]. Angular momentum transport is probably fairly effective in the convection envelope, and the usual approximation for such zones is to

assume solid-body rotation (Endal and Sofia 1981). We now consider what would happen if at first only the convective zone is spun down, a possibility indicated by the calculations of Endal and Sofia (1981). In this case we identify $I = I_c$, the moment of inertia of the convective envelope.

Because theories presently cannot predict the dependence of angular momentum loss on stellar parameters (cf. Mestel 1984), many different functional forms for $(\Delta J)R/I$ can be envisioned. Here we make the assumption that the variation of I_c/I_* provides the dominant mass dependence in the mass range of interest ($0.7 < M/M_\odot < 1.0$). For concreteness, we assume that $(\Delta J)R/I_*$ is independent of mass as well as rotation in this mass interval. In this case, the reduction in equatorial velocity predicted by equation (6) is directly proportional to I_*/I_c.

We once again adopt the initial distribution of rotational velocities shown in Figure 8 as a starting point. We also choose the normalization such that $(\Delta J)R/I_*\ (I_*/I_c) = 60$ km s^{-1} for 0.7 $M_\odot$ stars. This identifies Figure 11 explicitly with 0.7 $M_\odot$ dwarfs. Then we scale the results by the ratio I_*/I_c, using stellar evolutionary calculations for main-sequence stars kindly provided by D. VandenBerg. In doing this we are implicitly assuming that most of the spin-down occurs near the main sequence, so that the appropriate I_c to use is that of the zero-age main sequence (ZAMS) convective zone. Comparison between the Pleiades and α Per G dwarfs indicates substantial spin-down between 5×10^7 and 7×10^7 yr ages, in agreement with this model.

The results of these assumptions about spin-down are shown in Figures 12*a*–12*c* for $M = 0.8$, 0.9, and 1.0 $M_\odot$. The figures show a remarkably rapid decrease in the number of rapid rotators with increasing mass, a decline which is roughly comparable to that observed.

The above exercises are meant only as initial explorations of possible functional dependences of angular momentum loss. In the absence of better theoretical understanding of the spin-down process, there are not enough observational constraints available to choose between different possibilities. At present, we can only arrive at two conditional statements: (1) If star formation in the Pleiades is coeval, it is difficult to account for the large angular momentum spread observed among late-type stars with angular momentum loss that increases substantially with increasing rotation (for rotational velocities greater than about 10 km s^{-1}, anyway). (2) The distribution of rotation can be reproduced with a smoothly varying angular momentum loss as a function of spectral type in the G–K dwarf interval if only the convective envelope is spun down at first. Otherwise, large differences in angular momentum loss between G and K stars are required.

VI. DISCUSSION AND SUMMARY

We have obtained rotational velocities for a sufficiently large sample of low-mass stars in the Pleiades to derive a good measure of the distribution of rotational velocities as a function of mass. Although the major features of this distribution are unlikely to be changed by additional data, specific new observations could test certain aspects of our model. (1) The apparent sharpness of the transition from all slow rotators to a significant fraction of rapid rotators at $(V-I)_0 \approx 0.8$ is very much determined by the colors assigned to HII 625 and HII 738. With the adopted large reddening corrections, they become the two bluest rapid rotators. With smaller reddening corrections for these two stars, the break to rapid rotation would appear much sharper. It would be useful to obtain high signal-to-noise, moderate-resolution spectra of these stars over a large wavelength range in order to derive improved spectral

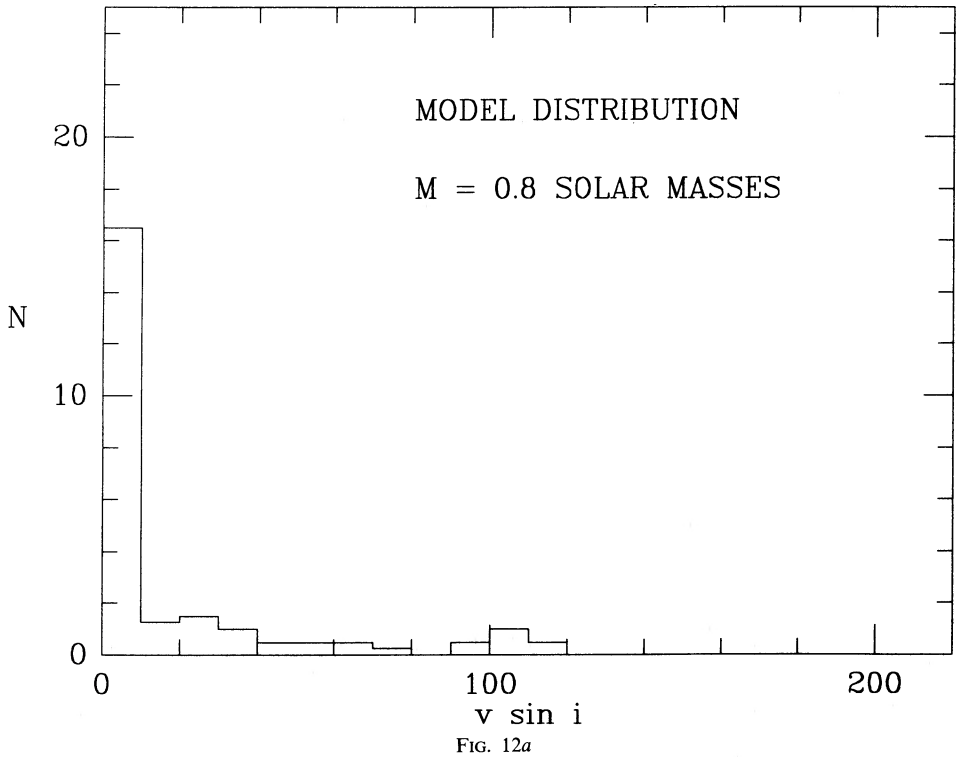

FIG. 12*a*

FIG. 12.—Same as Fig. 11, but for stars with mass approximately (*a*) 0.8, (*b*) 0.9, and (*c*) 1.0 $M_\odot$

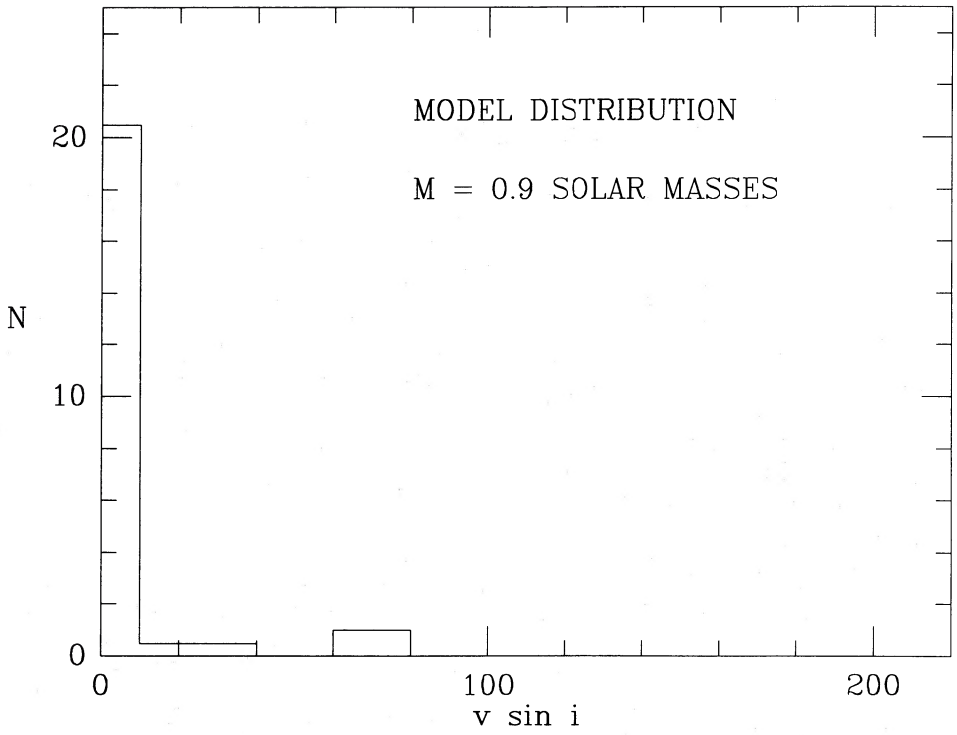

FIG. 12*b*

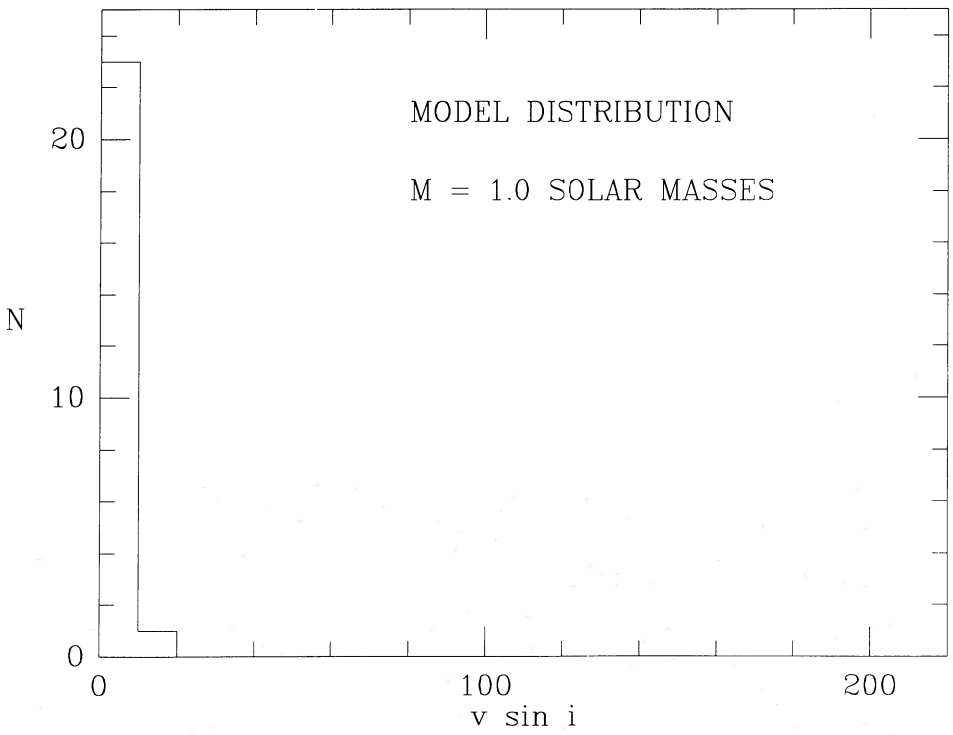

FIG. 12*c*

types (the inferred spectral type may be a function of wavelength, since both stars are likely to be heavily spotted). New optical photometry with careful attention to sky subtraction, possibly using a CCD, would also be useful, since both stars are located in regions contaminated by reflection nebulosity. (2) Higher resolution spectra of the Pleiades K dwarfs for which $v \sin i$ upper limits were derived should be obtained in order to determine the true range of rotational velocities. Similar data for the T Tauri stars with $v \sin i < 10$ km s^{-1} are needed also. (3) Additional spectra for stars with $V-I > 2.0$ should be obtained. These stars are important because of the dependence of the spin-down time scale on mass that we predict. The very red stars should have much longer spin-down time scales than the K dwarfs. A time spread of star formation that would significantly affect the observed rotational velocity distribution of the K dwarfs would have little effect on the distribution for the M dwarfs. Therefore, an accurate determination of the rotational velocity distribution for the red stars might allow us to discriminate among the various models for producing the rotational velocity distribution observed for the K dwarfs.

The models for explaining the Pleiades observations can also be tested by obtaining observations of other clusters. If well-sampled distributions for several clusters younger than the Hyades were obtained, the dependence of spin-down time scale on mass could be determined simply by comparing the different distributions. A well-sampled distribution for a cluster whose nuclear age is about 3×10^7 yr would be particularly useful. For such a cluster, the age spread of star formation could be estimated directly from the width of the pre–main-sequence track in a color-magnitude diagram.

We thank R. Mathieu for allowing us to derive rotational velocity estimates for a number of stars from spectra he obtained for another program. We also thank R. Hewett for improvements to the rotational velocity analysis package, and J. Peters and E. Horine for obtaining some of the spectra.

REFERENCES

Abt, H. A., and Hunter, J. H. 1962, *Ap. J.*, **136**, 381.
Allen, C. W. 1976, *Astrophysical Quantities* (3d ed.; London: Athlone).
Andriesse, C. D., Piersma, Th. R., and Witt, A. A. 1977, *Astr. Ap.*, **54**, 841.
Arny, T. 1977, *Ap. J.*, **217**, 83.
Baliunas, S., *et al.* 1983, *Ap. J.*, **275**, 752.
Bouvier, J., Bertout, C., Benz, W., and Mayor, M. 1986, *Astr. Ap.*, **165**, 110.
Breger, M. 1985, preprint.
Caillault, J.-P., and Helfand, D. J. 1985, *Ap. J.*, **289**, 279.
Campbell, B. 1984, *Ap. J.*, **283**, 209.
Castelaz, M., Sellgren, K., and Werner, M. 1986, *Ap. J.*, **313**, 853.
Chaffee, F. 1974, *Ap. J.*, **189**, 427.
Cohen, M., and Kuhi, L. V. 1979, *Ap. J. Suppl.*, **41**, 743.
Conti, P. S., and Ebbets, D. 1977, *Ap. J.*, **213**, 438.
Crawford, D. L., and Perry, C. L. 1976, *A.J.*, **81**, 419.
Duncan, D. K., and Jones, B. F. 1983, *Ap. J.*, **271**, 663.
Dworetsky, M. M. 1974, *Ap. J. Suppl.*, **28**, 101.
Eggen, O. 1950, *Ap. J.*, **112**, 81.
———. 1975, *Pub. A.S.P.*, **87**, 107.
Endal, A., and Sofia, S. 1981, *Ap. J.*, **243**, 625.
Federman, S. R., and Willson, R. F. 1984, *Ap. J.*, **283**, 626.
FitzGerald, P. M. 1970, *Astr. Ap.*, **4**, 234.
Gray, D. 1984, *Ap. J.*, **281**, 719.
Haro, G., Chavira, E., and Gonzalez, G. 1982, *Bol. Inst. Tonantzintla*, **3**, 1.
Hartmann, L. W. 1985, *Solar Phys.*, **100**, 587.
Hartmann, L. W., Hewett, R., Stahler, S., and Mathieu, R. 1986, *Ap. J.*, **309**, 275. (HHSM)
Hartmann, L. W., and Kenyon, S. 1986, preprint.
Hartmann, L. W., Soderblom, D., Noyes, R., Burnham, J., and Vaughan, A. 1984, *Ap. J.*, **276**, 254.
Hartmann, L., and Stauffer, J. 1987, in preparation.
Herbig, G. H. 1962, *Ap. J.*, **135**, 736.
Hertzsprung, E. 1947, *Ann. Leiden Obs.*, **19**, No. 1A.
Johnson, H. L., and Mitchell, R. I. 1958, *Ap. J.*, **128**, 31.
Jones, B. F. 1981, *A.J.*, **86**, 290.
Kraft, R. 1967, *Ap. J.*, **150**, 551.
———. 1970, in *Spectroscopic Astrophysics*, ed. G. H. Herbig (Berkeley: University of California Press), p. 385.
Kraft, R. P., and Greenstein, J. L. 1969, in *Low Luminosity Stars*, ed. S. Kumar (New York: Gordon & Breach), p. 65.
Kron, G., Gascoigne, S., and White, H. 1957, *A.J.*, **62**, 205.
Landolt, A. 1973, *A.J.*, **78**, 959.
———. 1979, *Ap. J.*, **231**, 468.
Latham, D. 1981, in *IAU Colloquium 67, Instrumentation for Astronomy with Large Optical Telescopes*, ed. C. M. Humphries (Dordrecht: Reidel), p. 259.
Marcy, G. W., Duncan, D. K., and Cohen, R. D. 1985, *Ap. J.*, **288**, 259 (MDC).
Mathieu, R. 1985, private communication.
———. 1986, in preparation.
McCarthy, M. F., and Treanor, P. J. 1968, *Specola Astr. Vaticana Ric. Astr.*, **7**, 367.
Mendoza, V. E. E. 1965, *Bol. Obs. Tonantzintla y Tacubaya*, **4**, 3.
Mermilliod, J. 1984, private communication.
Mestel, L. 1984, in *Cool Stars, Stellar Systems and the Sun*, ed. S. L. Baliunas and L. Hartmann (Berlin: Springer), p. 49.
Meys, J. M., Alphenaar, P., and van Leeuwen, F. 1982, *Inf. Bull. Var. Stars*, No. 2115.
Norman, C., and Silk, J. 1980, *Ap. J.*, **238**, 158.
Noyes, R. W., Hartmann, L. W., Baliunas, S. L., Duncan, D. K., and Vaughan, A. H. 1984, *Ap. J.*, **279**, 763.
Pallavicini, R., Golub, L., Rosner, R., Vaiana, G., Ayres, T., and Linsky, J. 1981, *Ap. J.*, **248**, 279.
Radick, R., Duncan, D., Baggett, W. E., Thompson, D. T., and Lockwood, G. W. 1986, private communication.
Rose, J. A. 1985, *A.J.*, **89**, 1238.
Rydgren, A. E., Vrba, F. J., Chugainov, P. F., and Shakhovskaya, N. I. 1985, *Bull. AAS*, **17**, 556.
Skumanich, A. 1972, *Ap. J.*, **171**, 565.
Slettebak, A. 1954, *Ap. J.*, **119**, 146.
———. 1955, *Ap. J.*, **121**, 653.
Smith, M. 1979, *Pub. A.S.P.*, **91**, 737.
Soderblom, D. 1983, *Ap. J. Suppl.*, **53**, 1.
———. 1985, *A.J.*, **90**, 2103.
Stauffer, J. 1980, *A.J.*, **85**, 1341.
———. 1982, *A.J.*, **87**, 1507.
———. 1984, *Ap. J.*, **280**, 189.
Stauffer, J., Dorren, J. D., and Africano, J. 1986, *A.J.*, **91**, 1443.
Stauffer, J., and Hartmann, L. 1986, *Ap. J. Suppl.*, **61**, 531.
Stauffer, J., Hartmann, L., Burnham, J. N., and Jones, B. F. 1985, *Ap. J.*, **289**, 247 (SHBJ).
Stauffer, J., Hartmann, L., and Latham, D. 1986, preprint.
Stauffer, J., Hartmann, L., Soderblom, D., and Burnham, J. 1984, *Ap. J.*, **280**, 202 (SHSB).
Stauffer, J., Ianna, P., McNamara, B., Jones, B. F., and Hartmann, L. 1986, in preparation.
Tonry, J., and Davis, M. 1979, *A.J.*, **84**, 1511.
VandenBerg, D. 1986, private communication.
van Leeuwen, F., and Alphenaar, P. 1982, *ESO Messenger*, No. 28, p. 15.
van Leeuwen, F., Alphenaar, P., and Brand, J. 1986, *Astr. Ap. Suppl.*, **165**, 999.
Vogel, S., and Kuhi, L. 1981, *Ap. J.*, **245**, 960.
Vrba, F. J., Rydgren, A. E., Zak, D. S., Chugainov, P. F., and Shakhovskaya, N. I. 1984, *Bull. AAS*, **16**, 998.
Walter, F. M. 1982, *Ap. J.*, **253**, 745.
White, R. E. 1984, *Ap. J.*, **284**, 1984.
Wilson, O. C. 1966, *Ap. J.*, **144**, 695.
Wolff, S. C., Edwards, S., and Preston, G. W. 1982, *Ap. J.*, **252**, 322.
Zappala, R. 1972, *Ap. J.*, **172**, 57.

LEE W. HARTMANN: Harvard-Smithsonian Center for Astrophysics, 60 Garden Street, Cambridge, MA 02138

JOHN R. STAUFFER: NASA/Ames Research Center, MS 245–6, Moffett Field, CA 94035